Electronic Supplementary Information (ESI)

Magnetic Anisotropy in Trigonal Planar Fe(II) Bis(trimethylsilyl)amido Complexes of the Type $[Fe\{N(SiMe_3)_2\}_2L]$ — Experiment and Theory

Tilmann Bodenstein,*[a,b] Andreas Eichhöfer,*[,a]

[a] Institut für Nanotechnologie, Karlsruher Institut für Technologie (KIT), Campus Nord, Hermann-von-Helmholtz-Platz 1, 76344 Eggenstein-Leopoldshafen, Germany

Tel. 49-(0)721-608-26371

Fax: 49-(0)721-608-26368

e-mail: andreas.eichhoefer@kit.edu

[b] present address: Hylleraas Center, Department of Chemistry, University of Oslo, P. O. Box 1033, 0315 Oslo, Norway; former address: Theoretical Chemistry, Department of Chemistry, Aarhus University, Langelandsgade 140, 8000 Aarhus C, Denmark

Content

List of compounds:

(1) $[Fe(N(SiMe_3)_2)_2(PPh_3)]$

(**2**) $[Fe(N(SiMe_3)_2)_2(PMe_3)]$

(**3**) $[Fe(N(SiMe_3)_2)_2(AsPh_3)]$

(**4**) $[Fe(N(SiMe_3)_2)_2(OPPh_3)]$

(**5**) $[Fe(N(SiMe_3)_2)_2(Py)]$

(**6**) $[Fe(N(SiMe_3)_2)_2(THF)]$

(**7**) $[Fe(N(SiMe_3)_2)_2(PCy_3)]$

Equations for the simulation of the dc and ac magnetic data

Simulations of the experimental dc magnetic data were performed with the PHI program [1] diagonalizing a spin Hamiltonian in the form

$$H = H_{CF} + H_{ZEE} \qquad \text{(S1)}$$

$$H_{CF} = \sum_{k=2} \sum_{q=-k}^{k} B_k^q O_k^q$$

$$H_{ZEE} = \mu_B \vec{S} \boldsymbol{g} \vec{B}$$

D: axial zero-field splitting (ZFS) parameter

$$D = 3B_2^0$$

E: rhombic ZFS parameter

$$E = B_2^2$$

$\vec{S}$: spin vector

$\vec{B}$: magnetic field vector

$\boldsymbol{g}$: g-tensor

μ_B: Bohr magneton

In all cases, the goodness of fit R for a particular data set is calculated following the least squares approach.

Relaxation times τ and the distribution coefficient α of the relaxation processes at a given temperature were derived from simultaneous fits of the frequency dependent curves of χ' and χ'' vs ν according to:[2]

$$\chi'(\omega) = \chi_S + \frac{(\chi_T - \chi_S)[1 + (\omega\tau)^{1-\alpha} \sin(\alpha\pi/2)]}{1 + 2(\omega\tau)^{1-\alpha} \sin(\alpha\pi/2) + (\omega\tau)^{2(1-\alpha)}} \qquad \text{(S2)}$$

$$\chi''(\omega) = \frac{(\chi_T - \chi_S)(\omega\tau)^{1-\alpha} \cos(\alpha\pi/2)}{1 + 2(\omega\tau)^{1-\alpha} \sin(\alpha\pi/2) + (\omega\tau)^{2(1-\alpha)}} \qquad \text{(S3)}$$

with

$\omega = 2\pi\nu$ angular frequency

χ_T = isothermal susceptibility

χ_S = adiabatic susceptibility

τ = magnetization relaxation time

$0 < \alpha < 1$ = width of the distribution of relaxation processes; ($\alpha = 0$; single relaxation process)

The field dependence of τ can be modeled by:[2,3]

$$\tau^{-1} = AH^2T + \frac{B_1}{1+B_2H^2} \quad \text{(S4)}$$

A: parameter of the direct relaxation mechanism

H: external dc field

T: temperature

B_1, B_2: parameters of the quantum tunneling mechanism

The preexponetial factor τ_0 and the effective energy U_{eff} of the spin reversal barrier were deduced from a linear fit of $\ln\tau$ against the inverse temperature T^{-1} according to:[4]

$$\ln\tau = \ln\tau_0 \frac{U_{eff}}{k}T^{-1} \quad \text{(S5)}$$

The temperature dependence of the relaxation times τ can be fit as a sum of contributions of the direct, Raman, quantum tunneling, and Orbach relaxation mechanism:[3,5]

$$\tau^{-1} = A_{Dir}T + \frac{B_1}{1+B_2H^2} + C_{Ram}T^5 + \frac{1}{\tau_0}\exp\left(\frac{-Ueff}{kT}\right) \quad \text{(S6)}$$

A_{Dir}: parameter of the direct relaxation mechanism

C_{Ram}: parameter of the Raman relaxation mechanism

U_{eff}: effective energy barrier

$$\Delta E_{av} = \frac{1}{5}\sum_{i=1}^{5} E_{corr}(i) \quad \text{(S7)}$$

Stevens operators used for decomposing the effective Hamiltonian in terms of Racah operators R(l,m) ($0 < m \leq l$):

$$O_l^{+m} = \frac{1}{\sqrt{2}K_l^m}\sqrt{\frac{2l+1}{4\pi}}(R_l^{-m} + (-1)^m R_l^m) \quad \text{(S8)}$$

$$O_l^0 = \frac{1}{K_l^0}\sqrt{\frac{2l+1}{4\pi}}R_l^0 \quad \text{(S9)}$$

$$O_l^{-m} = \frac{i}{\sqrt{2}K_l^m}\sqrt{\frac{2l+1}{4\pi}}\left(R_l^{-|m|} - (-1)^m R_l^{|m|}\right) \quad \text{(S10)}$$

Where the normalization coefficients *K*(l,m) of the real spherical harmonics are tabled, see, e. g. ref. 6.

The matrix elements of the Stevens operator equivalents can thus be computed from the Racah operators *R*(l,m), which are given in the pseudo spin basis using Wigner 3j symbols by

$$\langle S, M|R_l^m|S, M'\rangle = \frac{(-1)^{S-M}}{2^l}\begin{pmatrix} S & l & S \\ -M & m & M' \end{pmatrix}\sqrt{\frac{(2S+l+1)!}{(2S-l)!}} \quad \text{(S11)}$$

Table S1. Crystallographic Data for [Fe{N(SiMe$_3$)$_2$}$_2$(PPh$_3$)] (**1**), [Fe{N(SiMe$_3$)$_2$}$_2$(PMe$_3$)] (**2**), [Fe{N(SiMe$_3$)$_2$}$_2$(AsPh$_3$)] (**3**) and [Fe{N(SiMe$_3$)$_2$}$_2$(OPPh$_3$)] (**4**) and [Fe{N(SiMe$_3$)$_2$}$_2$(py)] (**5**).

			1	**2**	**3**	**4**	**5**
sum formula			$C_{30}H_{51}FeN_2PSi_6$	$C_{15}H_{45}FeN_2PSi_4$	$C_{30}H_{51}AsFeN_2Si_4$	$C_{30}H_{51}FeN_2OPSi_4$	$C_{30}H_{51}FeN_2OPSi_4$
fw [g/mol]			638.9	452.71	682.85	654.90	455.74
crystal system			triclinic	orthorhombic	triclinic	monoclinic	orthorhombic
space group			*P*–1	*Pna*2(1)	*P*–1	*P*2(1)/*c*	*P*2(1)2(1)2
Cell	*a*	[pm]	1010.5(2)	1831.6(4)	1008.44(5)	1217.9(2)	1104.57(3)
	b		1333.3(3)	1059.9(2)	1347.94(6)	1540.6(3)	34.230(1)
	c		1372.4(3)	1431.3(3)	1382.94(7)	2029.4(4)	1068.70(3)
	α		90.46(3)		90.654(4)		
	β	[°]	93.70(3)		93.729(4)	96.63(3)	
	γ		91.07(3)		91.626(4)		
V [10^6pm^3]			1844.7(6)	2778.6(10)	1874.95(16)	3782.3(13)	4040.7(2)
Z			2	4	2	4	6
T [K]			180(2)	180(2)	183(2)	180(2)	200(2)
d_c [g cm^{-3}]			1.150	1.082	1.210	1.150	1.124
$\mu(\lambda)$ [mm^{-1}]			0.602	0.774	1.426	0.591	0.744
F[000]			684	984	720	1400	1476
$2\theta_{max}$ [°]			55.5	53.5	53.5	53.5	51
meas reflns			19114	15898	18246	37719	15719
unique reflns			7790	5717	7864	8018	7119
R_{int}			0.0455	0.0583	0.0431	0.0549	0.0659
reflns with $I > 2\sigma(I)$			5774	3748	6671	5508	6171
refined params			509	224	503	367	359
$R1(I > 2\sigma(I))$[a]			0.0361	0.0393	0.0328	0.0431	0.0438
*wR*2(all data)[b]			0.0782	0.0913	0.0871	0.1167	0.1143
abs. struct. parameter				0.46(4)			0.40(2)

[a] $R1 = \Sigma||F_o| - |F_c||/\Sigma|F_o|$. [b] $wR2 = \{\Sigma[w(F_o^2 - F_c^2)^2] / \Sigma[w(F_o^2)^2]\}^{1/2}$

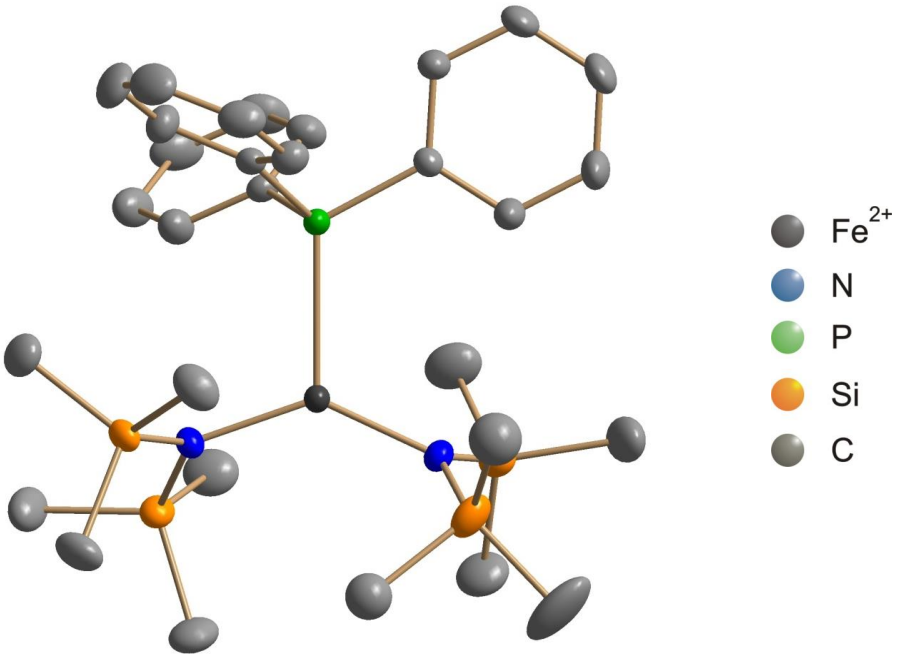

Figure S1. Molecular structure of [Fe(N(SiMe$_3$)$_2$)$_2$(PPh$_3$)] (**1**) in the crystal (ellipsoids drawn at 50% probability level, H atoms omitted).

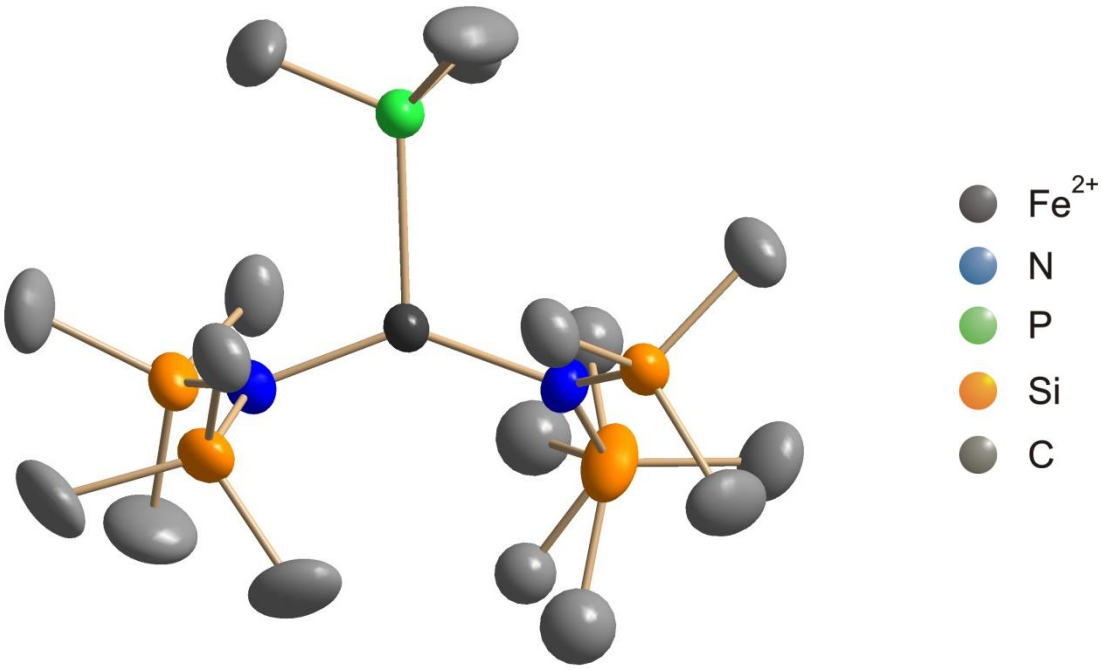

Figure S2. Molecular structure of [Fe(N(SiMe$_3$)$_2$)$_2$(PMe$_3$)] (**2**) in the crystal (ellipsoids drawn at 50% probability level, H atoms omitted).

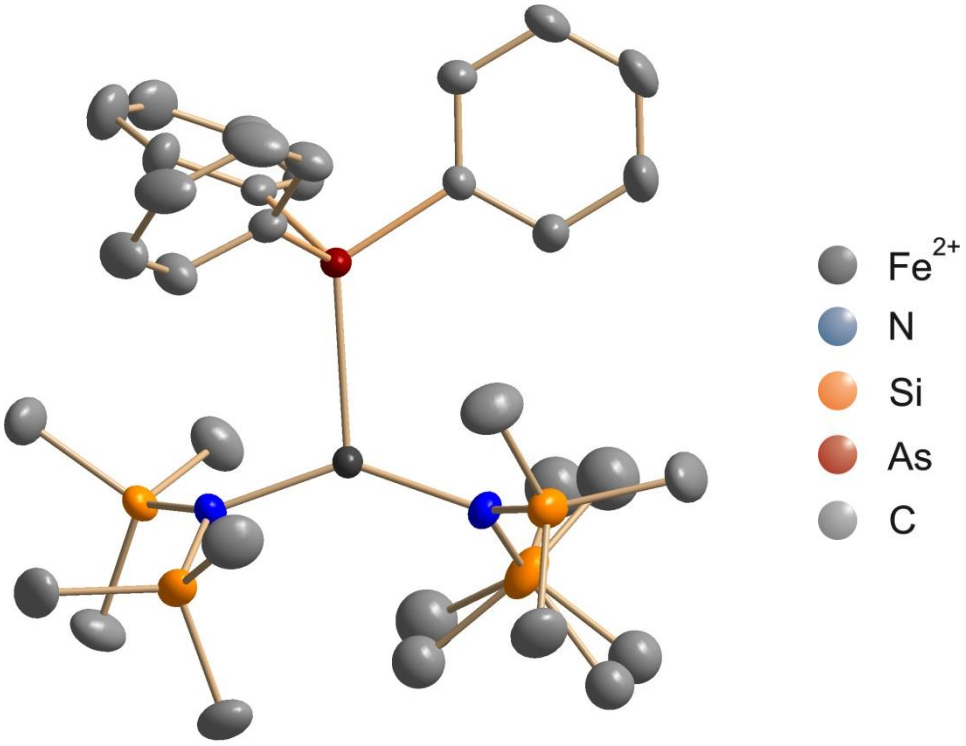

Figure S3. Molecular structure of [Fe(N(SiMe$_3$)$_2$)$_2$(AsPh$_3$)] (**3**) in the crystal (ellipsoids drawn at 50% probability level, H atoms omitted).

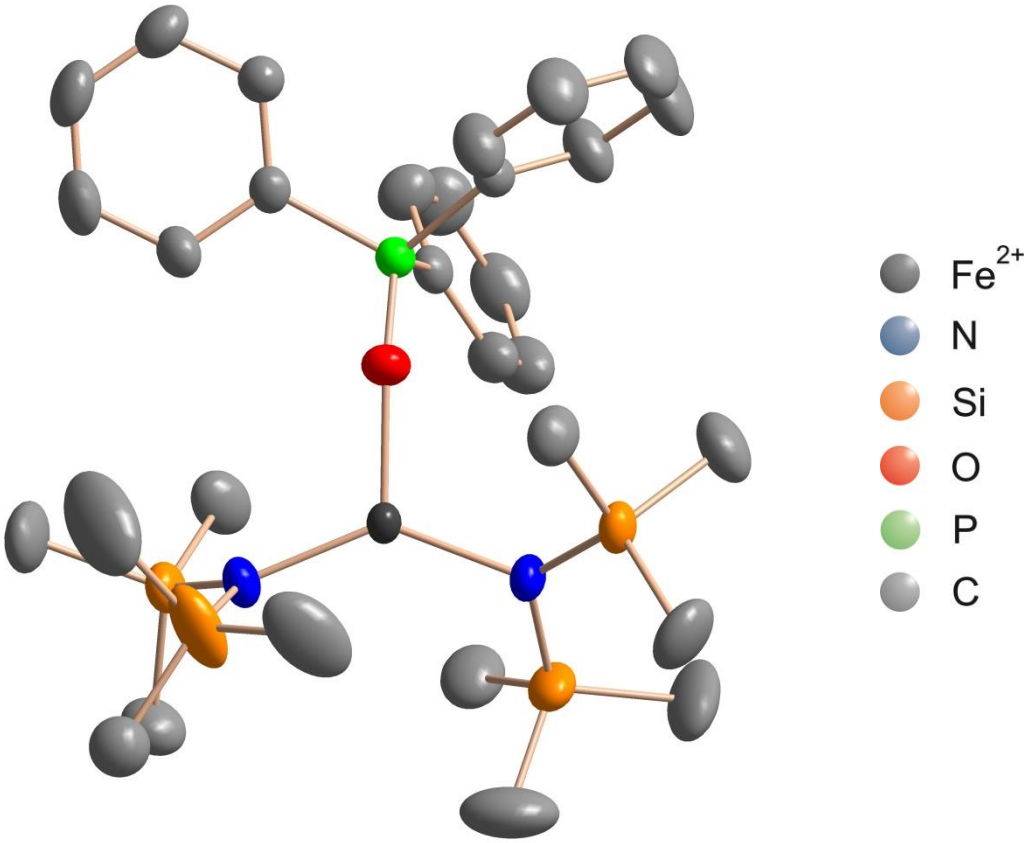

Figure S4. Molecular structure of [Fe(N(SiMe$_3$)$_2$)$_2$(OPPh$_3$)] (**4**) in the crystal (ellipsoids drawn at 50% probability level, H atoms omitted).

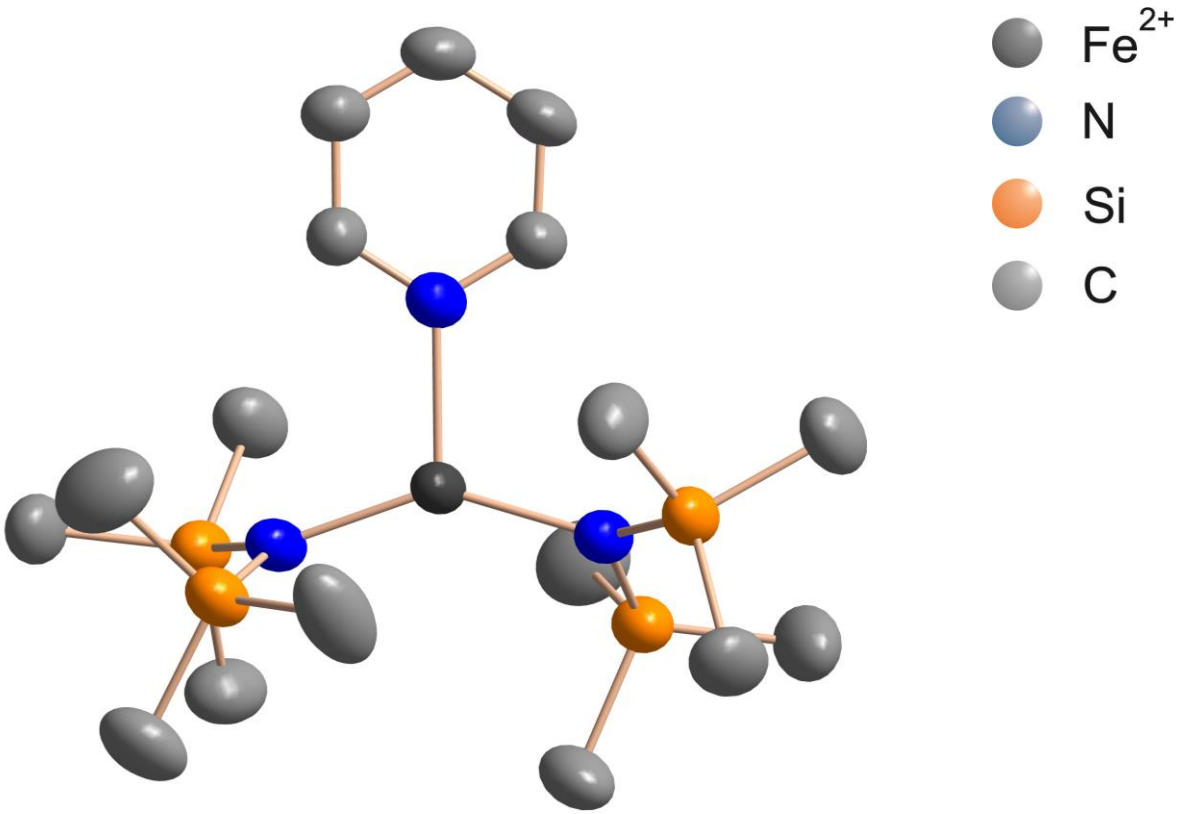

Figure S5. Molecular structure of [Fe(N(SiMe$_3$)$_2$)$_2$(py)] **5a** in the crystal structure of **5** (ellipsoids drawn at 50% probability level, H atoms omitted).

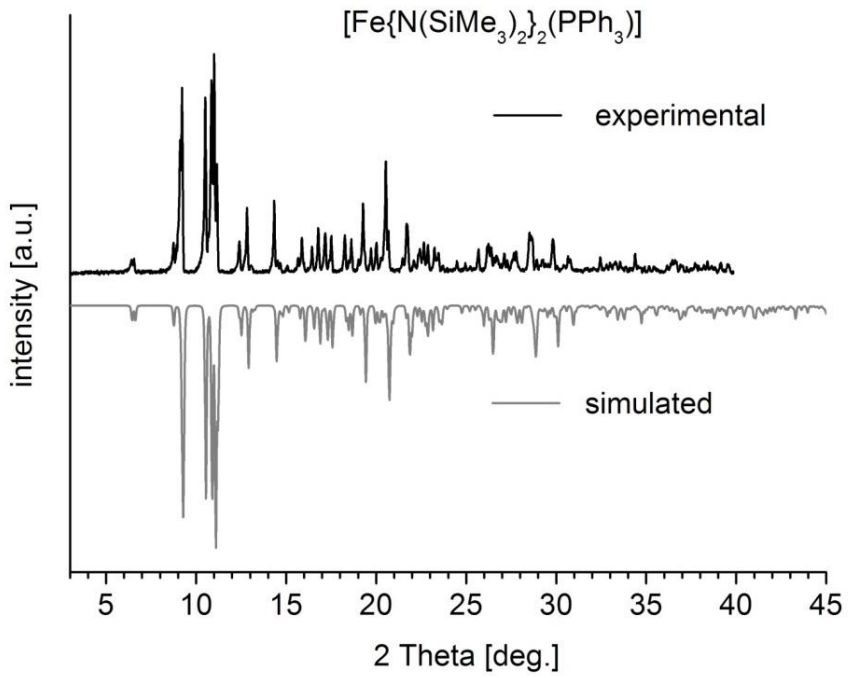

Figure S6. Measured (black) and simulated (grey) X–ray powder pattern for $[Fe\{N(SiMe_3)_2\}_2PPh_3]$ (**1**).

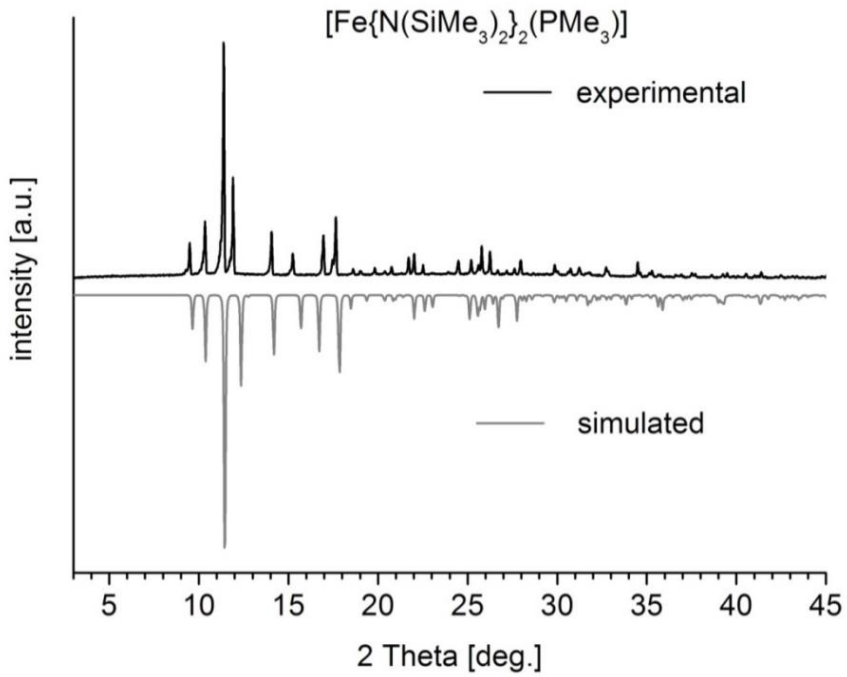

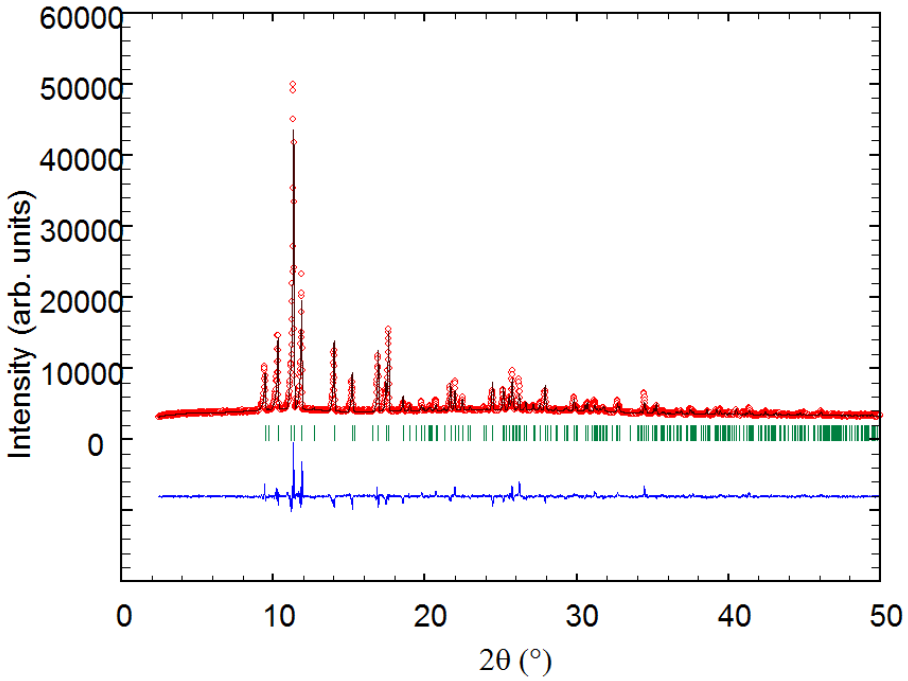

powder refinement data:

orthorhombic, *Pna*2_1

a = 18.651, b = 10.467, c = 14.882 Å

V = 2905.2 Å^3

Bragg R-factor: 14.6, RF-factor : 24.6

Figure S7. Measured (black) and simulated (grey) X–ray powder pattern for $[Fe\{N(SiMe_3)_2\}_2PMe_3]$ (**2**).

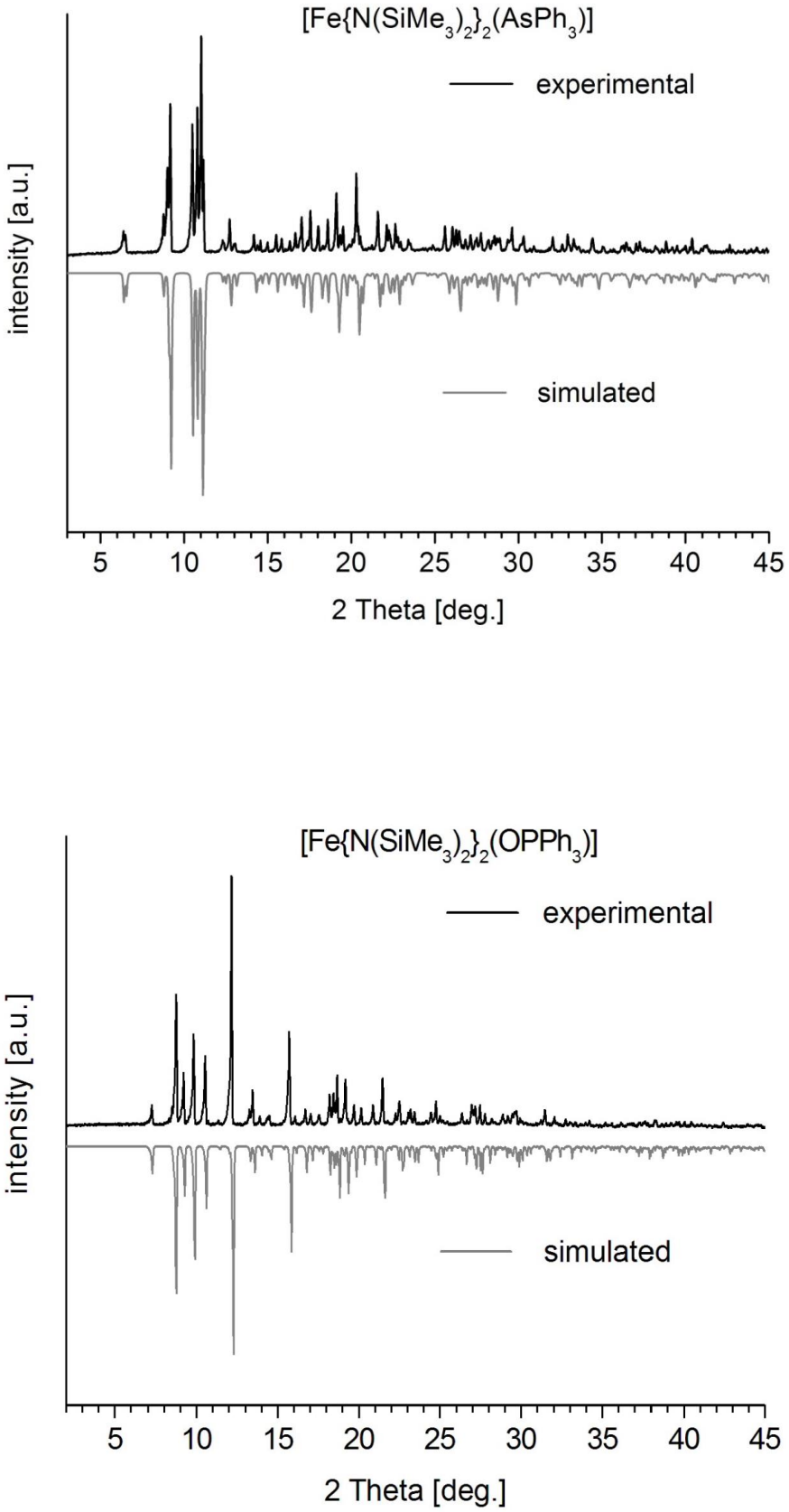

Figure S8. Measured (black) and simulated (grey) X–ray powder pattern for $[Fe\{N(SiMe_3)_2\}_2(AsPh_3)]$ (**3**) (up) and $[Fe\{N(SiMe_3)_2\}_2(OPPh_3)]$ (**4**) (below).

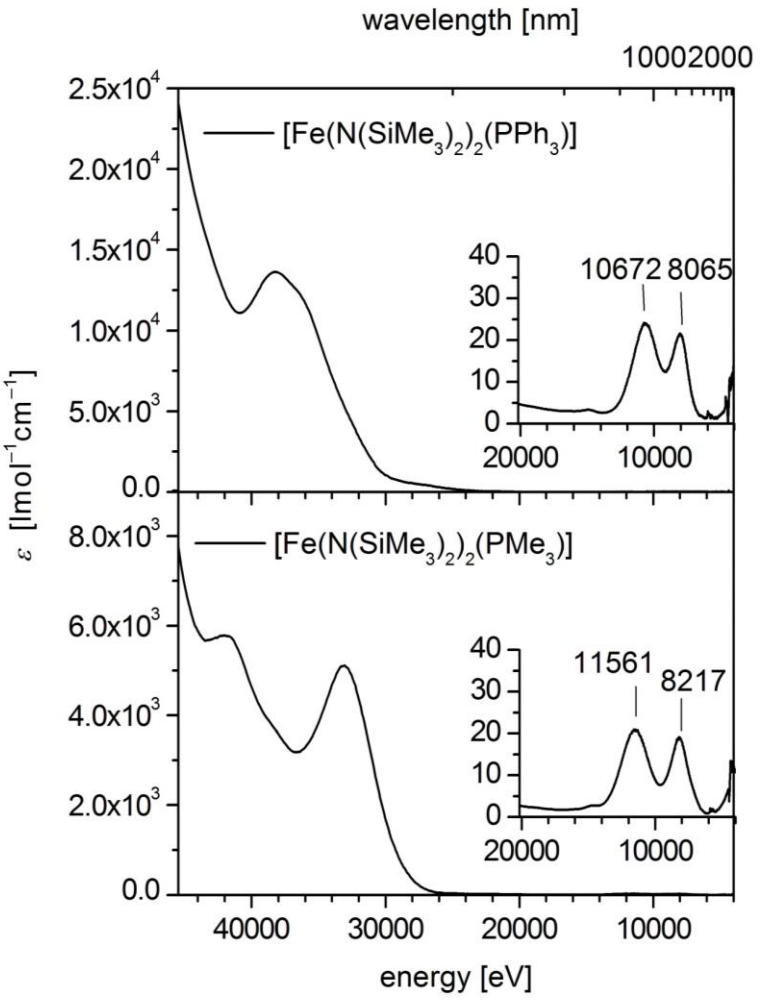

Figure S9. Electronic spectra of **1** and **2** in C_6D_6.

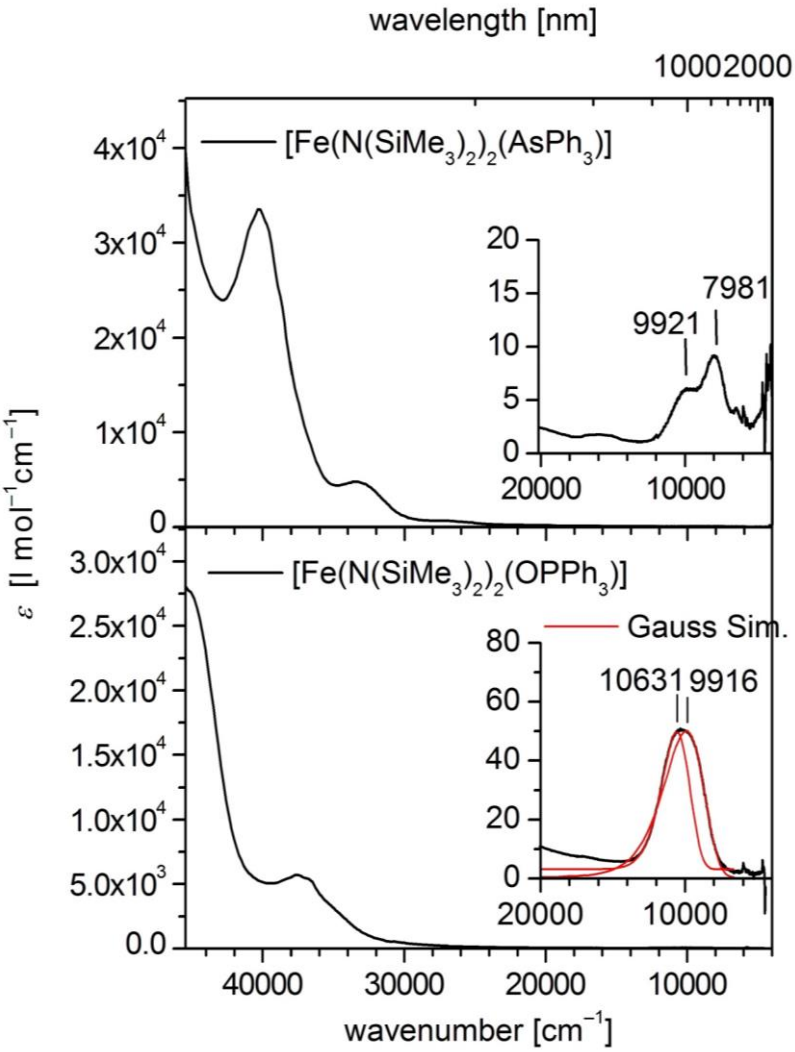

Figure S10. Electronic spectra of **3** and **4** in C_6D_6.

a)

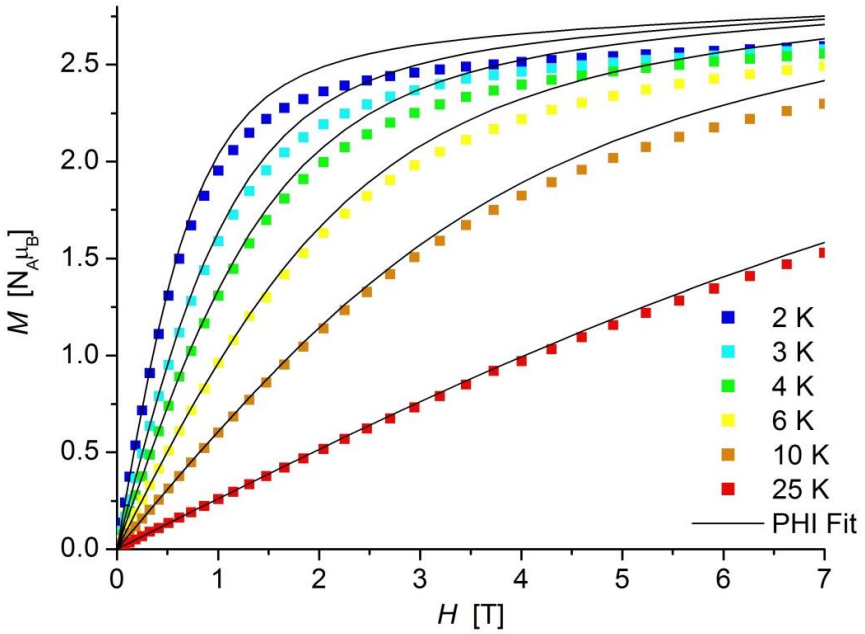

b)

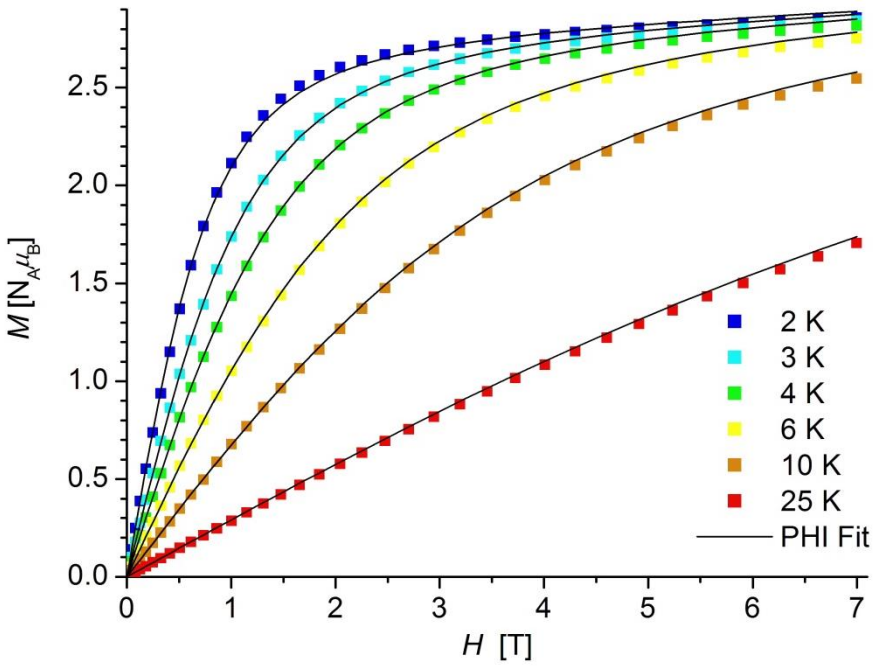

Figure S11. Plots of magnetization *M* versus *H* for a) [Fe{N(SiMe$_3$)$_2$}$_2$PPh$_3$] (**1**) and b) [Fe{N(SiMe$_3$)$_2$}$_2$PMe$_3$] (**2**) measured between 2 and 25 K. The solid lines represent the calculated curves (eqn (S1)) with the PHI program [1] (Table 2).

a)

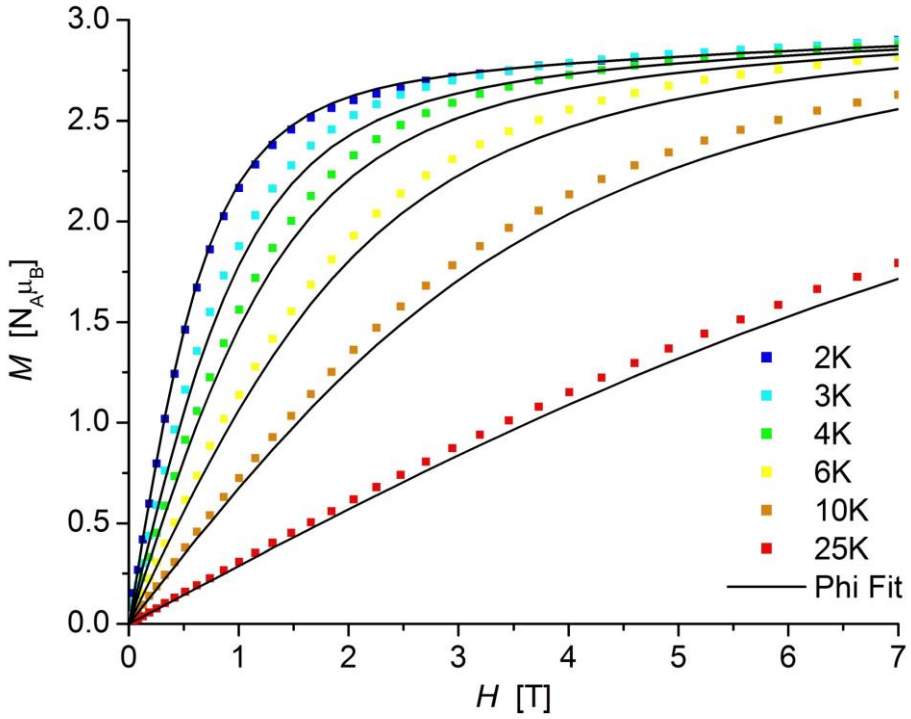

b)

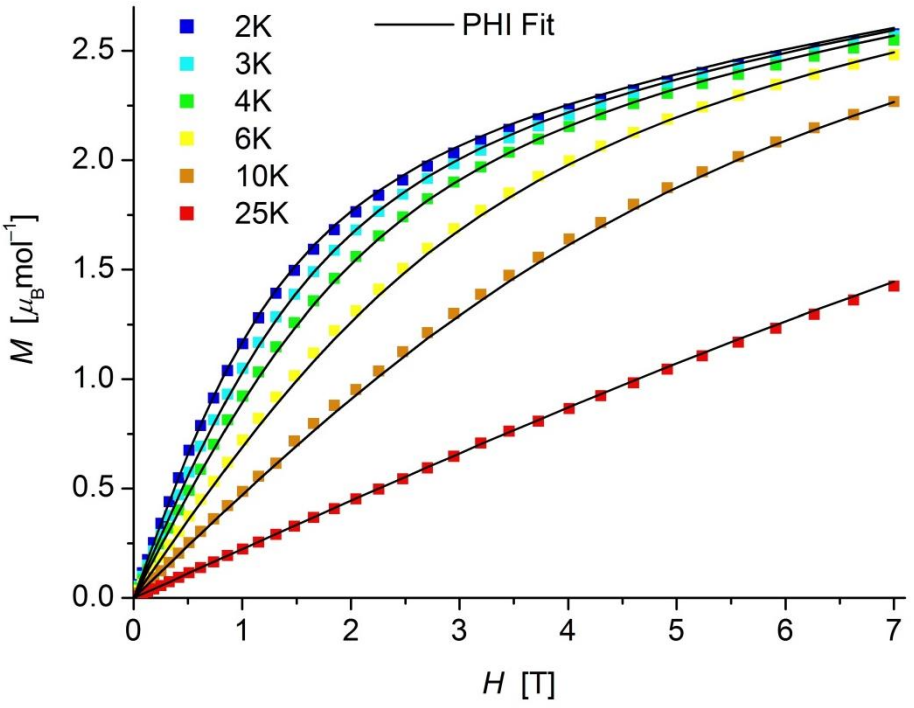

Figure S12. Plots of magnetization *M* versus *H* for a) $[Fe\{N(SiMe_3)_2\}_2AsPh_3]$ (**3**) and b) $[Fe\{N(SiMe_3)_2\}_2OPPh_3]$ (**4**) measured between 2 and 25 K. The solid lines represent the calculated curves (eqn (S1)) with the PHI program [1] (Table 2).

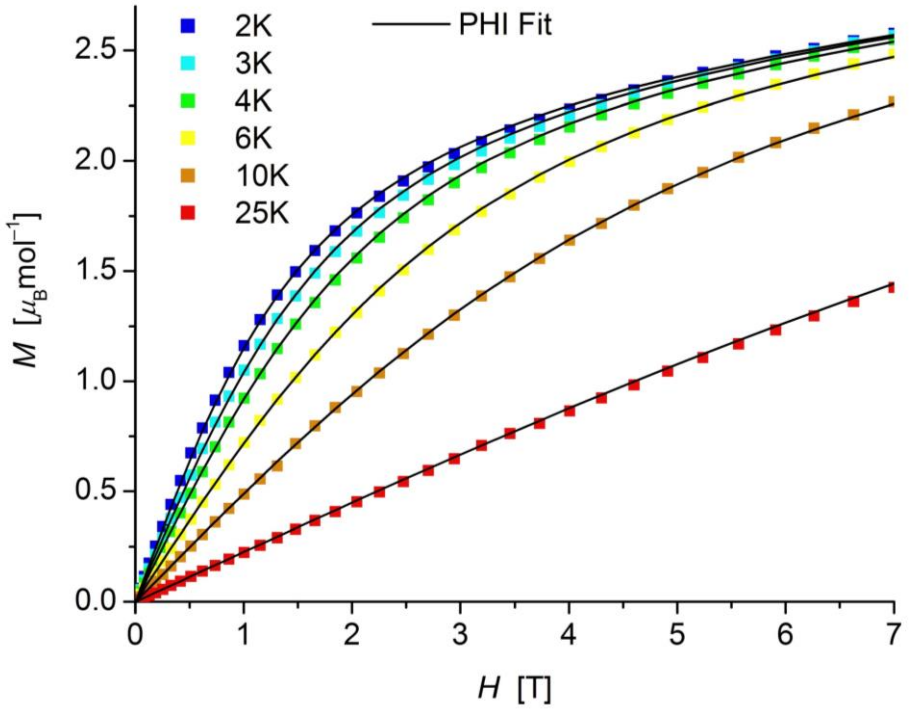
2K
3K
4K
6K
10K
25K
PHI Fit
M [μB mol-1]
H [T]
0.0
0.5
1.0
1.5
2.0
2.5
0
1
2
3
4
5
6
7

a)

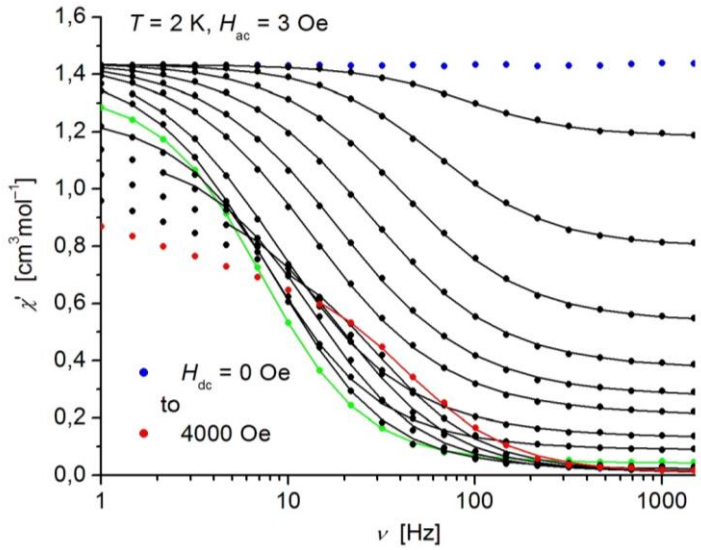

b)

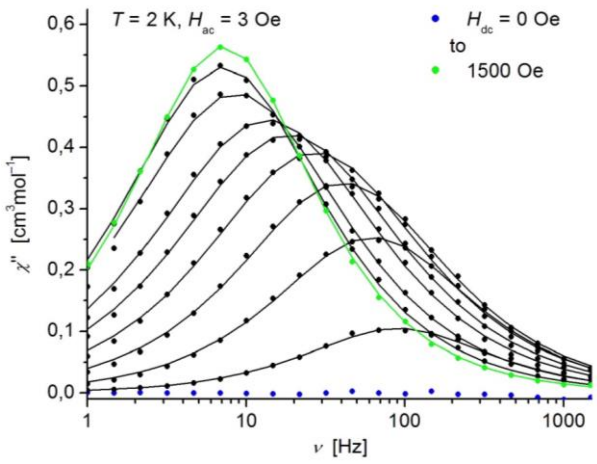

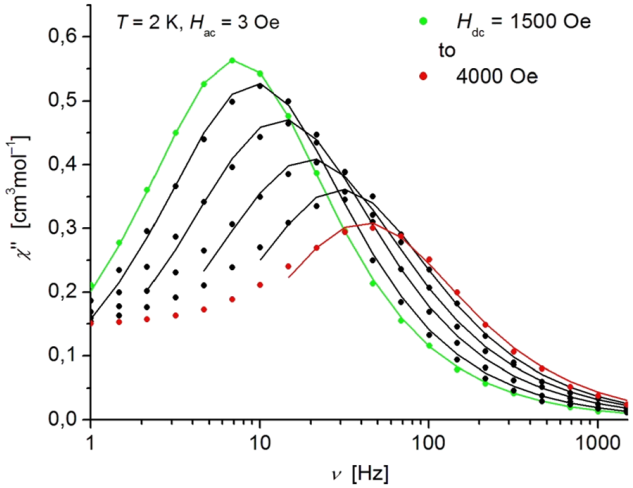

Figure S13. Frequency dependence of the in-phase χ' (a) and out-of-phase χ'' (b) component of the ac magnetic susceptibility at 2K under different dc fields for $[Fe(N(SiMe_3)_2)_2(PPh_3)]$ (**1**) (solid lines correspond to the fits to a distribution of single relaxation processes (eqns (S2) and (S3), SI)).

a)

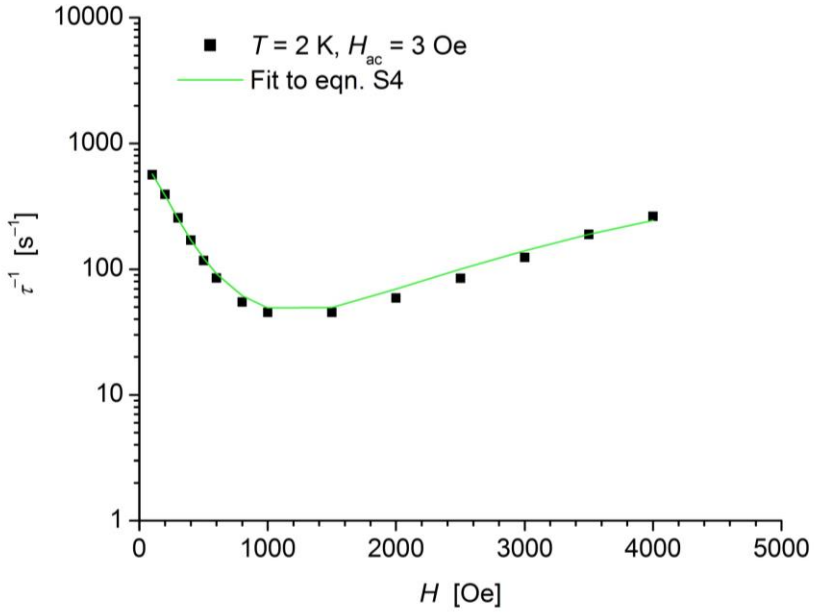

b)

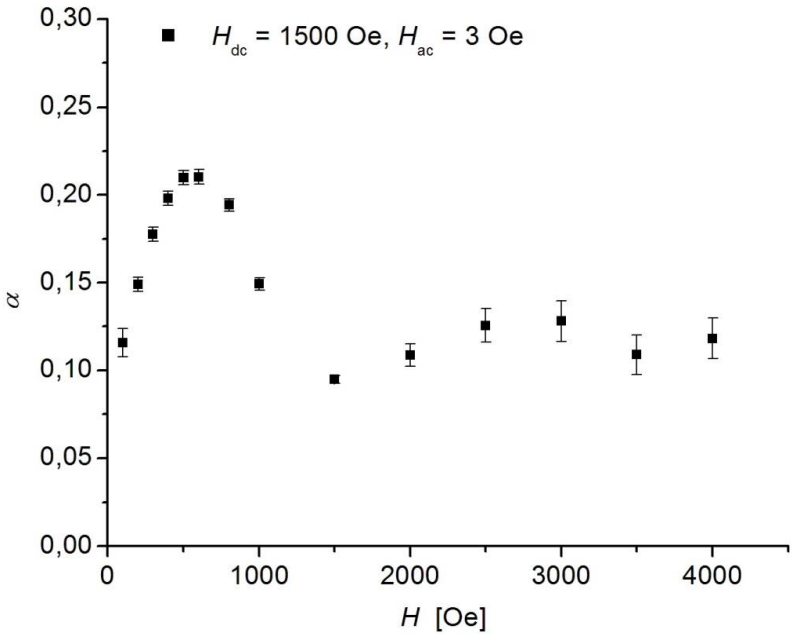

Figure S14. a) Field dependence of the inverse relaxation time τ^{-1} at T = 2 K for [Fe(N(SiMe$_3$)$_2$)$_2$(PPh$_3$)] (**1**). The green line corresponds to the fit according to eqn (S4). Respective parameters are listed in Table S2 b) Field dependence of the distribution coefficient α at T = 2 K extracted from the fits are shown in Figure S13.

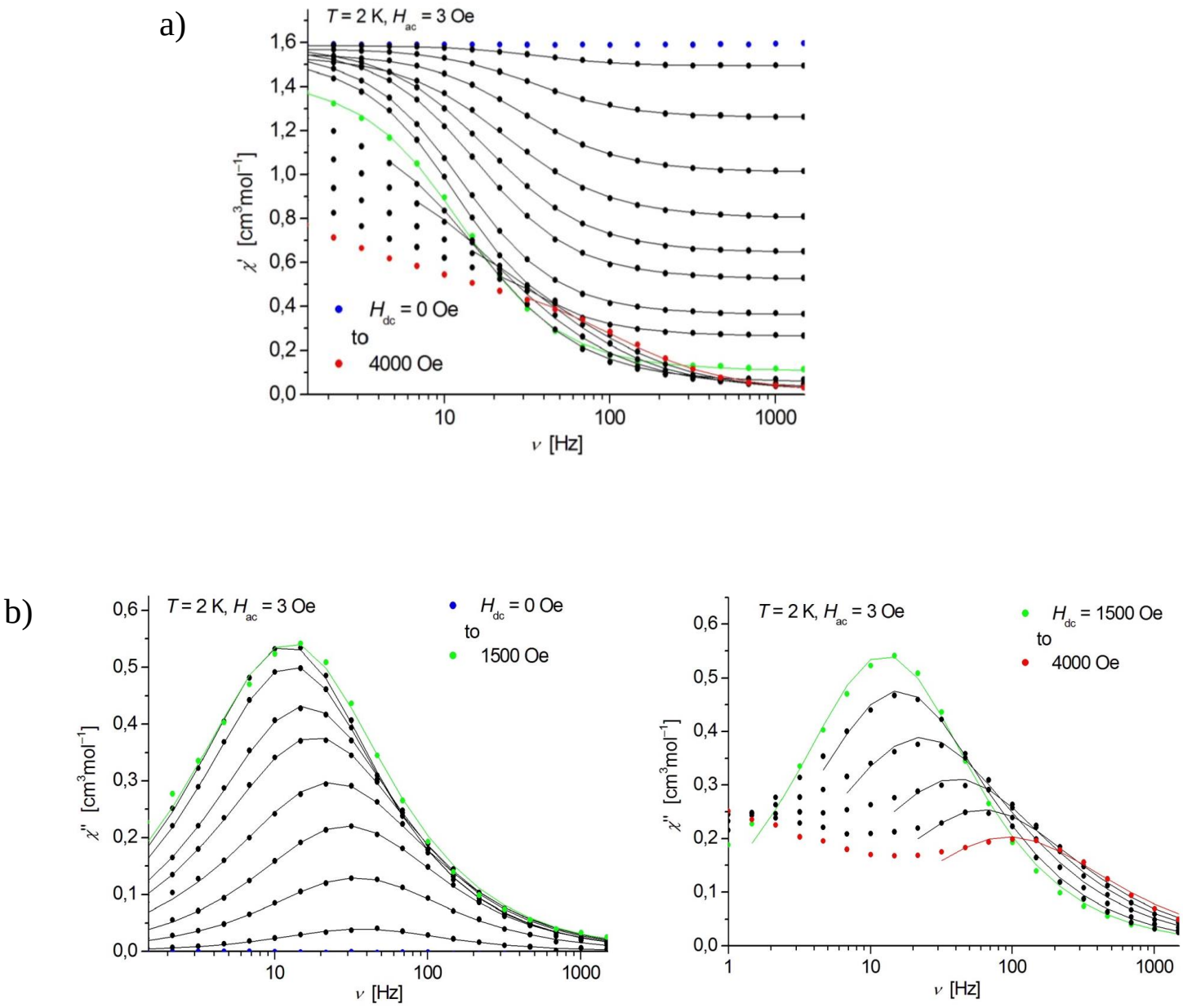

Figure S15. Frequency dependence of the in-phase χ' (a) and out-of-phase χ'' (b) component of the ac magnetic susceptibility at 2K under different dc fields for $[Fe(N(SiMe_3)_2)_2(PMe_3)]$ (**2**) (solid lines correspond to the fits to a distribution of single relaxation processes (eqns (S2) and (S3), SI)).

a)

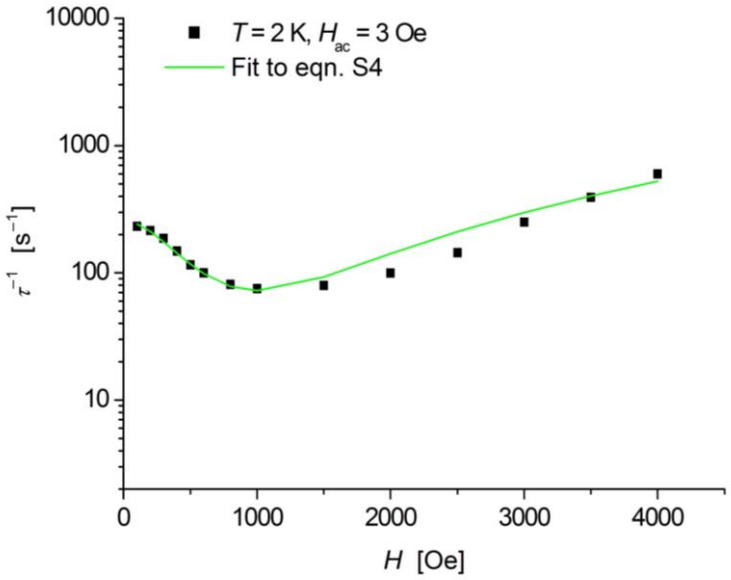

b)

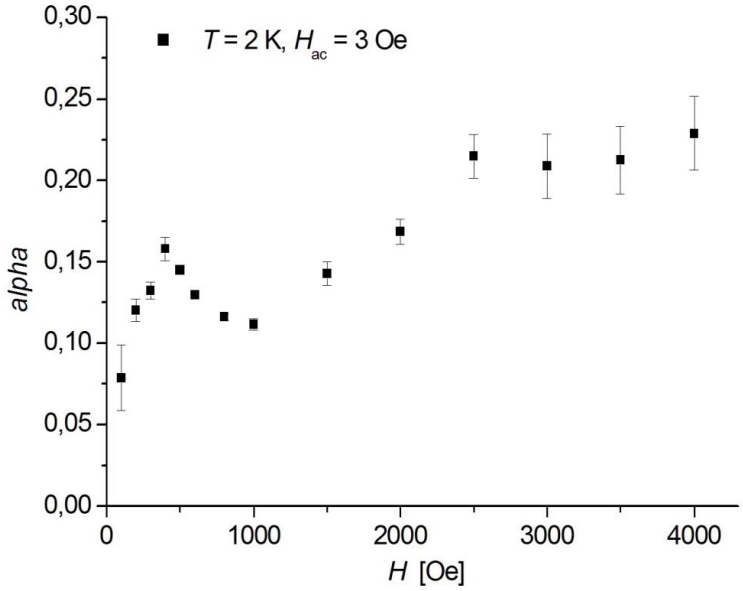

Figure S16. a) Field dependence of the inverse relaxation time τ^{-1} at T = 2 K for [Fe(N(SiMe$_3$)$_2$)$_2$(PMe$_3$)] (**2**). The green line corresponds to the fit according to eqn (S4). Respective parameters are listed in Table S2 b) Field dependence of the distribution coefficient α at T = 2 K extracted from the fits shown in Figure S15.

a)

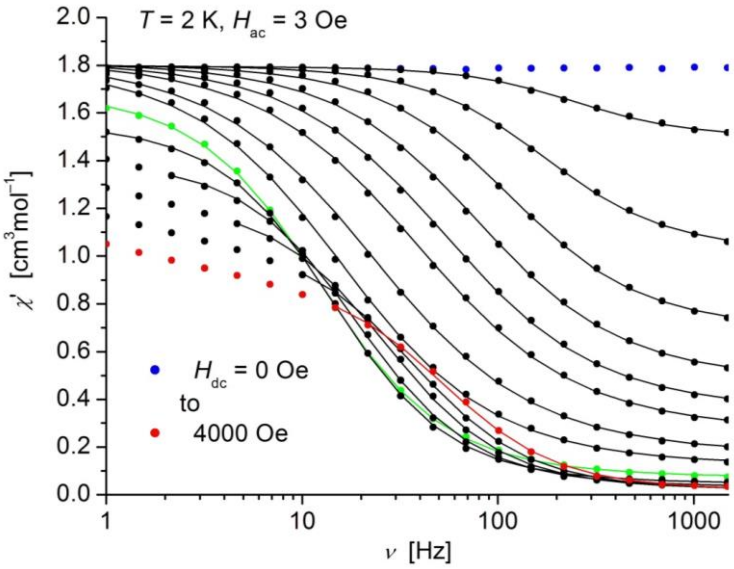

b)

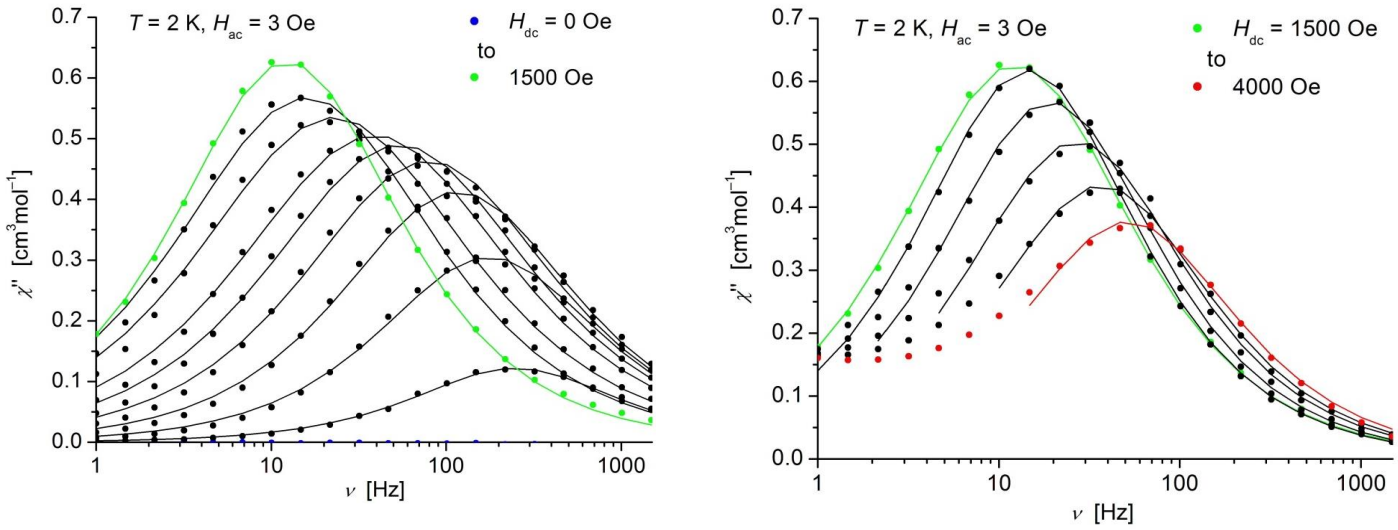

Figure S17. Frequency dependence of the in-phase χ' (a) and out-of-phase χ'' (b) component of the ac magnetic susceptibility at 2K under different dc fields for $[Fe(N(SiMe_3)_2)_2(AsPh_3)]$ (**3**) (solid lines correspond to the fits to a distribution of single relaxation processes (eqns (S2) and (S3)).

a)

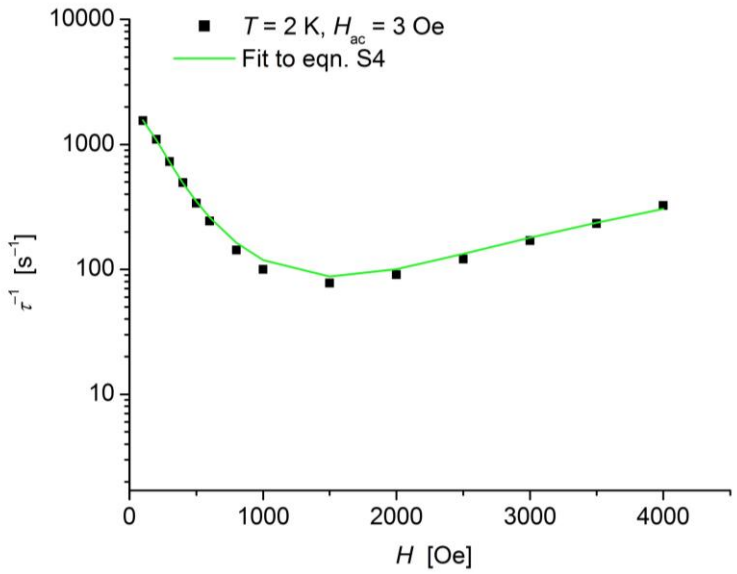

b)

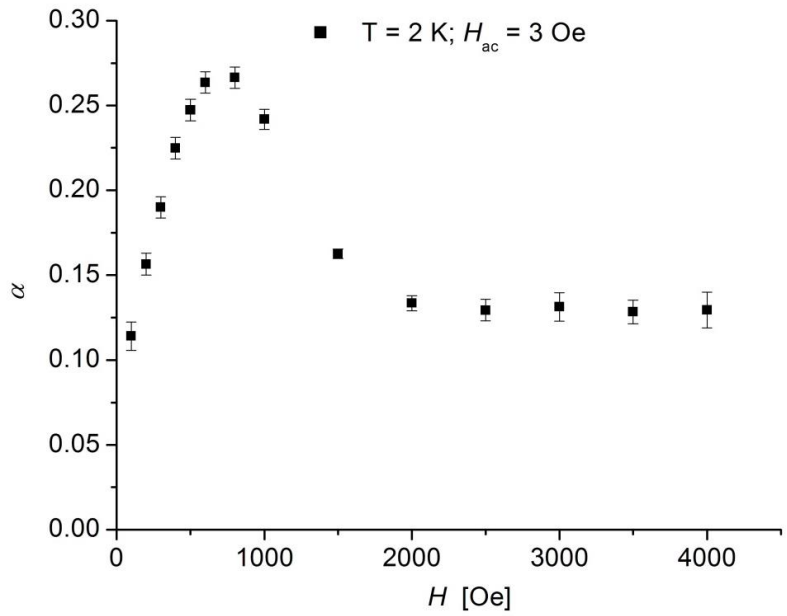

Figure S18. a) Field dependence of the inverse relaxation time τ^{-1} at T = 2 K for [Fe(N(SiMe$_3$)$_2$)$_2$(AsPh$_3$)] (**3**). The green line corresponds to the fit according to eqn (S4). Respective parameters are listed in Table S2 b) Field dependence of the distribution coefficient α at T = 2 K extracted from the fits shown in Figure S17.

Table S2 Results of the fittings of the field dependent ac magnetic data of **1**–**3** [a]

	A [$s^{-1}Oe^{-2}$]	B_1 [s^{-1}]	B_2 [Oe^{-2}]
1	$2.0(1) \cdot 10^{-5}$	677(17)	$2.0(1) \cdot 10^{-5}$
2	$3.0(2) \cdot 10^{-5}$	255(35)	$5.4(22) \cdot 10^{-6}$
3	$2.0(1) \cdot 10^{-5}$	1836(22)	$2.0(1) \cdot 10^{-5}$

[a] According to eqn (S4) (Figure S14a, S16a and S18a)

a)

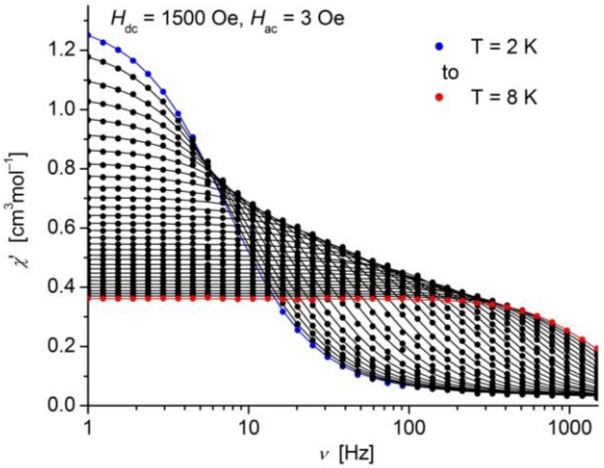

b)

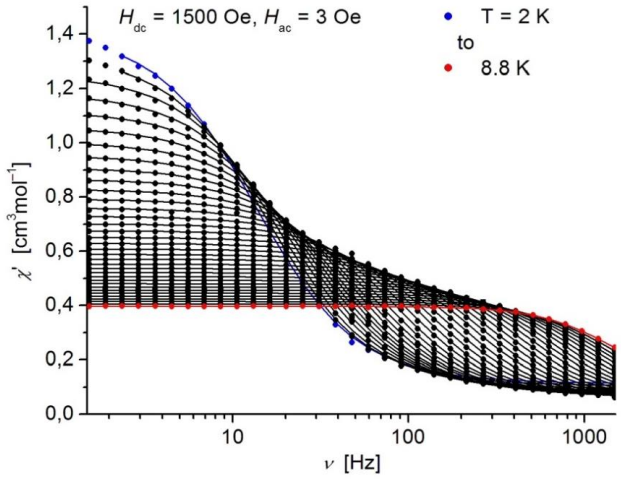

c)

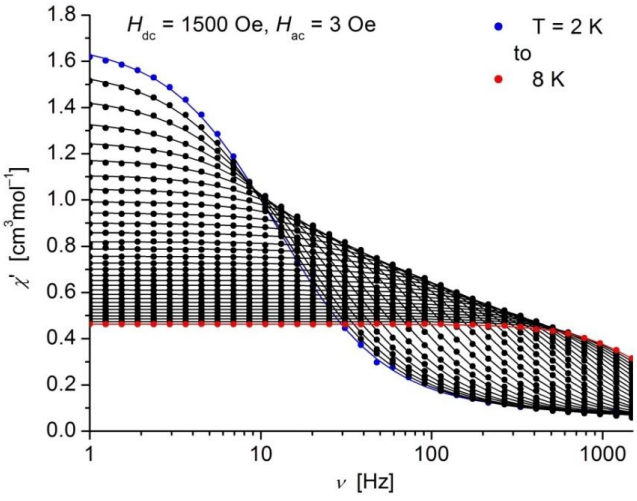

Figure S19. Frequency dependence of the in-phase χ' component of the ac magnetic susceptibility at 1500 Oe at different temperatures for **1**–**3** (a–c). Solid lines represent the fits according to eqn (S2) and (S3).

a)

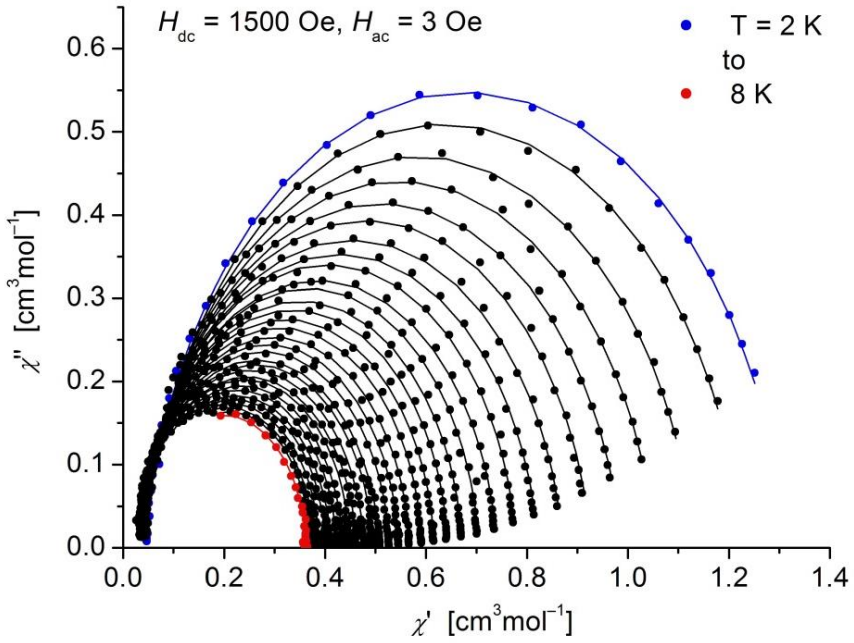

b)

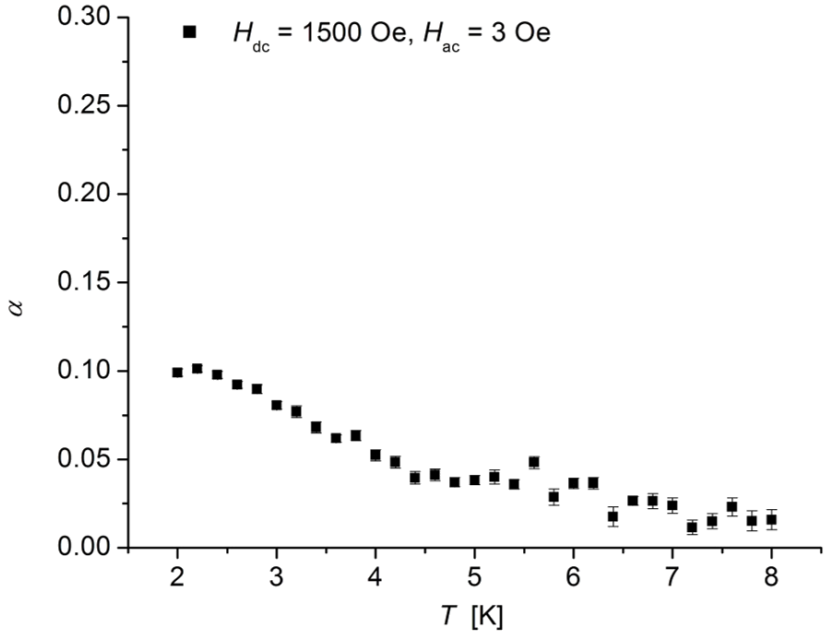

Figure S20. a) Cole-Cole plots for χ'' vs χ' of [Fe{N(SiMe$_3$)$_2$}$_2$PPh$_3$] (**1**) at different temperatures. The solid lines correspond to the fits obtained with a Debye model (eqn (S2) and (S3)) from which also the distribution coefficients α (plotted in b)) for the relaxation processes were determined.

a)

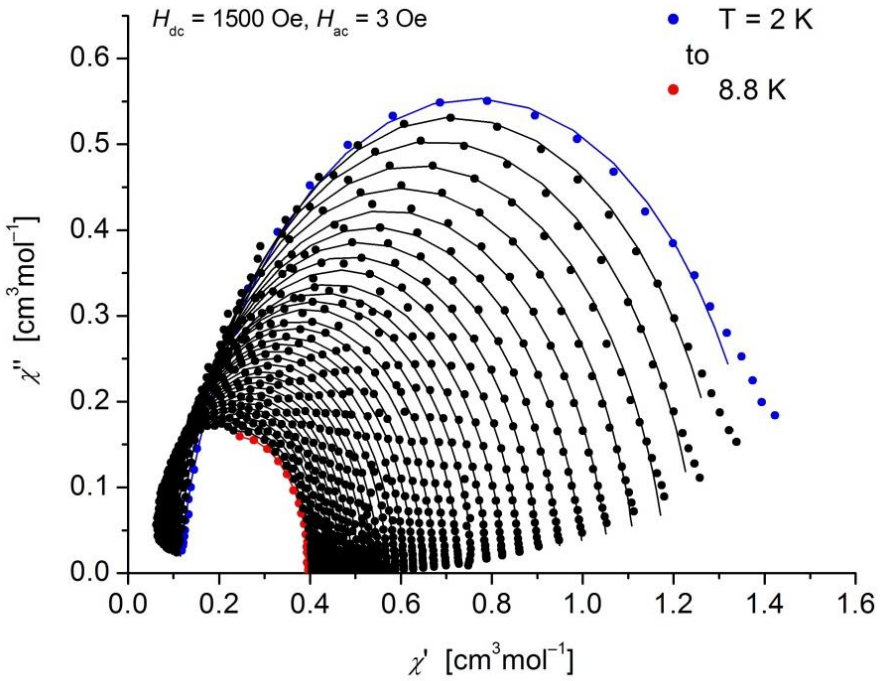

b)

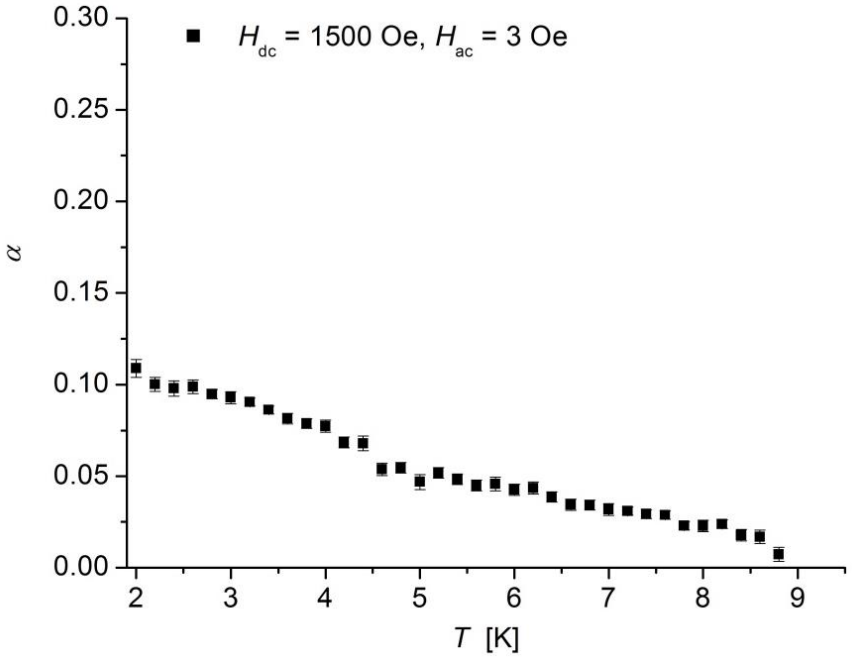

Figure S21. a) Cole-Cole plots for χ'' vs χ' of [Fe{N(SiMe$_3$)$_2$}$_2$PMe$_3$] (**2**) at different temperatures. The solid lines correspond to the fits obtained with a Debye model (eqn (S2) and (S3)) from which also the distribution coefficients α (plotted in b)) for the relaxation processes were determined.

a)

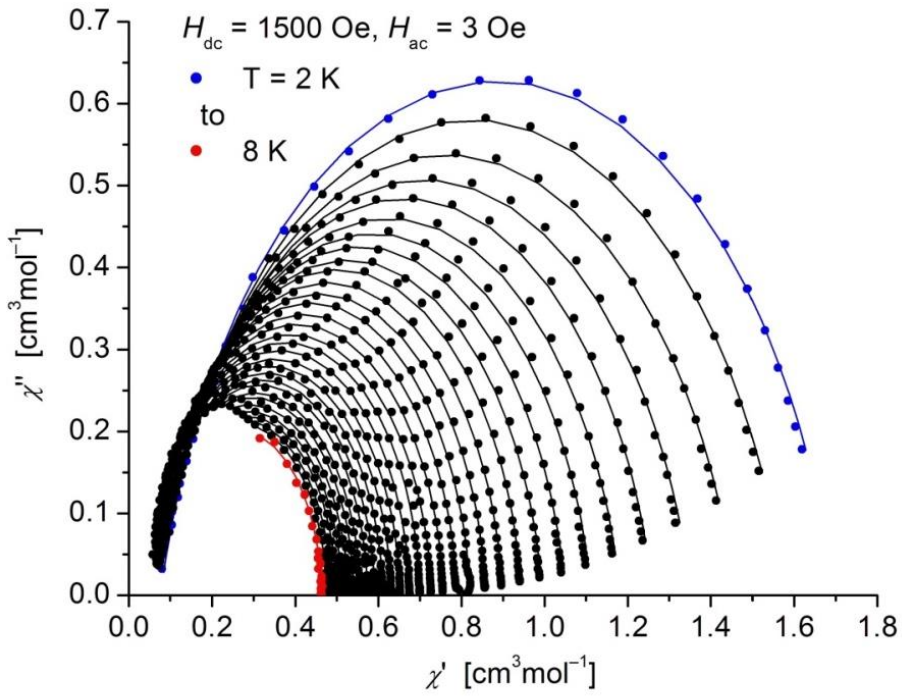

b)

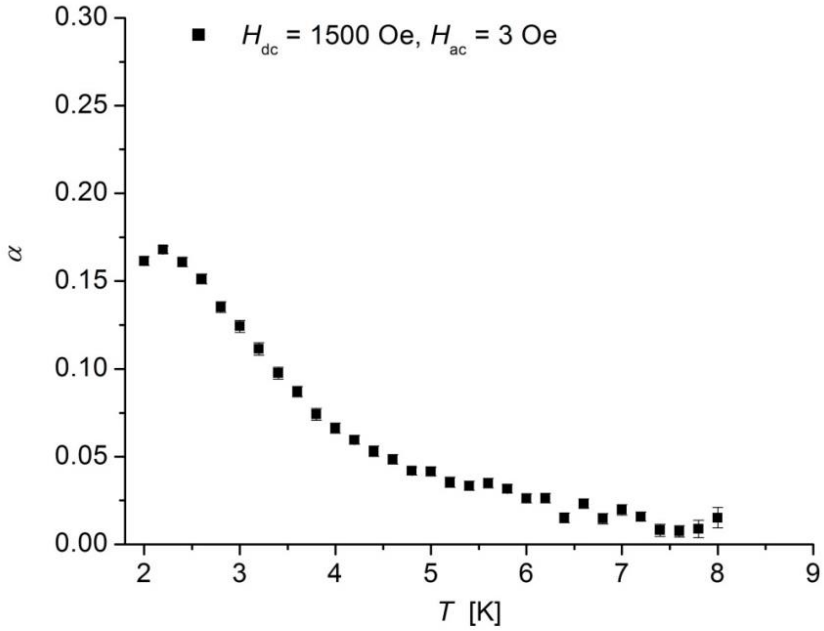

Figure S22. a) Cole-Cole plots for χ'' vs χ' of [Fe{N(SiMe$_3$)$_2$}$_2$AsPh$_3$] (**3**) at different temperatures. The solid lines correspond to the fits obtained with a Debye model (eqn (S2) and (S3)) from which also the distribution coefficients α (plotted in b)) for the relaxation processes were determined.

Table S3 Spin-Free energies (in cm^{-1}) of the lowest five quintet states of complexes **1**–**7** from ab initio calculations using different active spaces and comparison with the experimental values

	CAS(6,5)			CAS(12,13)						experiment
	SCF	PT2(ss)	PT2(ms)	CI [a]	SCF	PT2(ss)[b]	PT2 (ms)[b]	PT2(ss)[c]	PT2(ms)[c]	
1	0	0	0	0	0	0	0	30	266	
	311	146	201	916	540	580	564	0	0	
	3329	3723	3758	3900	3218	3887	3890	3691	3816	
	7679	7989	8024	9402	8316	9018	9042	7970	8094	8065
	10015	10436	10486	11803	10978	11358	11379	10599	10740	10672
2	0	0	0	0	0	0	0	0	0	
	413	243	232	433	192	264	271	335	344	
	3527	3953	3953	3549	4046	3844	3865	4045	4052	
	7775	8140	8141	7797	8420	7977	7977	9014	8995	8217
	10923	11357	11370	10944	11446	11307	11355	12515	12547	11561
3	0	0	0	0	0	27	262	18	253	
	392	194	180	617	176	0	0	0	0	
	3757	4426	4234	4586	3725	4063	4182	4062	4181	
	7749	8102	8109	8878	7692	7945	8060	7946	8061	7981
	9783	9913	9958	12105	10357	9736	9875	9735	9873	9921
4	0	0	0	0	0			0	0	
	858	1332	1342	1021	2133			1668	1673	
	2801	3437	3448	3161	3519			3401	3403	
	8422	9233	9244	8540	9414			9759	9670	9916
	10283	11035	11057	11240	11767			11167	11273	10631
5a [d]					0			0	0	
					1123			651	661	
					3468			3563	3574	
					8253			8400	8368	
					12244			11315	11377	
5b [d]					0			0	0	
					1186			749	758	
					3316			3400	3410	
					8779			8987	8971	
					12428			11563	11607	
6 [d]					0			0	0	
					1395			887	897	
					3657			3613	3622	
					8801			9214	9224	8631
					11346			10527	10549	10083
7 [e]	0	0	0	0	0	0	234	0	309	
	298	172	171	422	187	27	0	33	0	
	2993	3390	3394	3468	3166	3383	3487	3249	3386	
	7634	7861	7866	9279	7529	7773	7877	8433	8576	8308
	9818	10463	10476	11466	10785	10302	10410	10592	10735	10728

[a] Based orbitals of the CAS(6,5)SCF calculation which where localized such that the doubly occupied ligand lone pairs pointing towards the iron center, as well as the double d-shell are in the active space.
[b] Number of localized, inactive orbitals in the vicinity of Fe, N, O, P kept (using Mulliken charge threshold of 0.10): 3 (**1**), 6 (**2**), 7 (**3**), 8 (**4**), 6 (**5**), 7 (**6**), 7 (**7**).
[c] Number of localized, inactive orbitals in the vicinity of Fe, N, O, P kept (using Mulliken charge threshold of 0.01 (0.00 for **3**)): 8 (**1**), 25 (**2**), 81 (**3**), 22 (**4**), 27 (**5**).
[d] Given the similarity of the results for **1**–**5**, only the CAS(12,13) based results with a Mulliken charge threshold of 0.01 for the PT2 calculations are shown.
[e] The root-flipping encountered going from PT2(SS) to PT2(MS) is difficult to access given the complexity of the multi-state, multi-reference perturbation theory. Note, however, that spin orbit coupling largely overcompensates this effect (Table S4).

Table S4 Spin-orbit coupled RASSI energies (cm^{-1}) of the lowest 11 states of complexes **1**–**7** based on CAS(12,13)SCF wave functions with and without CASPT2 energy corrections to the spin-orbit configuration interaction matrix

	1			**2**			**3**			**4**		
(12,13)	CAS	SSPT2	MSPT2	CAS	SSPT2	MSPT2	CAS	SSPT2	MSPT2	CAS	SSPT2	MSPT2
1	0	0	0	0	0	0	0	0	0	0	0	0
2	0	0	0	0	0	0	0	0	0	5	4	4
3	154	137	136	99	166	146	158	172	152	20	27	27
4	158	141	140	116	168	151	164	173	157	46	53	53
5	255	210	208	153	324	232	264	337	243	47	57	56
6	436	533	539	701	344	486	444	352	490	2172	1724	1728
7	521	589	594	738	487	554	535	504	565	2176	1732	1736
8	553	622	627	757	518	588	560	530	593	2196	1748	1752
9	694	747	750	859	671	722	710	689	734	2221	1782	1786
10	695	748	751	859	672	723	710	689	735	2224	1784	1788
11	4305	4260	4264	3393	4021	4053	4001	4405	4429	3587	3480	3482

	5a			**5b**			**6**			**7**		
(12,13)	CAS	SSPT2	MSPT2	CAS	SSPT2	MSPT2	CAS	SSPT2	MSPT2	CAS	SSPT2	MSPT2
1	0	0	0	0	0	0	0	0	0	0	0	0
2	2	1	1	3	1	1	3	2	2	0	0	0
3	48	82	81	44	72	71	37	61	61	153	169	142
4	72	102	101	69	93	93	61	83	83	160	170	148
5	83	129	127	79	115	114	68	100	99	255	320	222
6	1211	788	797	1269	873	881	1467	994	1004	447	360	523
7	1227	818	827	1284	898	906	1479	1016	1025	533	497	585
8	1241	833	841	1298	913	921	1491	1029	1038	562	529	619
9	1296	920	927	1351	991	998	1535	1096	1104	708	685	750
10	1297	920	927	1352	991	998	1536	1096	1105	709	685	751
11	3571	3712	3722	3418	3538	3546	3745	3733	3742	3440	3589	3621

Table S5 RASSI wave function analysis/decomposition of **1** – **7**. Weights of the three most important spin–orbit–free states for the lowest ten spin–orbit states.

(1) $[Fe(N(SiMe_3)_2)_2(PPh_3)]$

SO State	energy [cm^{-1}]	Spin–free state	Spin	Weights	Spin–free state	Spin	Weights	Spin–free state	Spin	Weights
CASSCF										
1	0	1	2.0	0.8131	2	2.0	0.1845	3	2.0	0.0011
2	0	1	2.0	0.8115	2	2.0	0.1864	3	2.0	0.0008
3	154	1	2.0	0.9268	2	2.0	0.0652	3	2.0	0.0069
4	158	1	2.0	0.9147	2	2.0	0.0815	3	2.0	0.0029
5	255	1	2.0	0.9901	3	2.0	0.0064	2	2.0	0.0025
6	436	2	2.0	0.9938	3	2.0	0.0045	4	2.0	0.0005
7	521	2	2.0	0.9270	1	2.0	0.0638	3	2.0	0.0079
8	553	2	2.0	0.9163	1	2.0	0.0816	4	2.0	0.0006
9	694	2	2.0	0.8097	1	2.0	0.1853	3	2.0	0.0033
10	695	2	2.0	0.8105	1	2.0	0.1848	3	2.0	0.0030
SSCASPT2										
1	0	1	2.0	0.5229	2	2.0	0.4757	7	1.0	0.0003
2	0	1	2.0	0.5226	2	2.0	0.4760	7	1.0	0.0003
3	137	1	2.0	0.5485	2	2.0	0.4480	3	2.0	0.0022
4	141	1	2.0	0.5173	2	2.0	0.4792	3	2.0	0.0025
5	210	1	2.0	0.9817	2	2.0	0.0145	3	2.0	0.0025
6	533	2	2.0	0.9773	1	2.0	0.0165	3	2.0	0.0052
7	589	2	2.0	0.5146	1	2.0	0.4766	3	2.0	0.0075
8	622	2	2.0	0.5476	1	2.0	0.4510	4	2.0	0.0004
9	747	2	2.0	0.5212	1	2.0	0.4747	3	2.0	0.0025
10	748	2	2.0	0.5231	1	2.0	0.4731	3	2.0	0.0023
MSCASPT2										
1	0	1	2.0	0.6839	2	2.0	0.3146	7	1.0	0.0003
2	0	1	2.0	0.6839	2	2.0	0.3146	7	1.0	0.0003
3	136	1	2.0	0.8054	2	2.0	0.1914	3	2.0	0.0018
4	140	1	2.0	0.8013	2	2.0	0.1959	3	2.0	0.0017
5	208	1	2.0	0.9963	3	2.0	0.0021	4	2.0	0.0005
6	539	2	2.0	0.9910	3	2.0	0.0059	1	2.0	0.0020
7	594	2	2.0	0.7980	1	2.0	0.1923	3	2.0	0.0084
8	627	2	2.0	0.8035	1	2.0	0.1947	3	2.0	0.0007
9	750	2	2.0	0.6821	1	2.0	0.3137	3	2.0	0.0027
10	751	2	2.0	0.6846	1	2.0	0.3117	3	2.0	0.0022

(**2**) $[Fe(N(SiMe_3)_2)_2(PMe_3)]$

SO State	energy [cm^{-1}]	Spin–free state	Spin	Weights	Spin–free state	Spin	Weights	Spin–free state	Spin	Weights
CASSCF										
1	0	1	2.0	0.6380	2	2.0	0.3606	6	1.0	0.0003
2	0	1	2.0	0.6380	2	2.0	0.3606	6	1.0	0.0003
3	99	1	2.0	0.7435	2	2.0	0.2536	3	2.0	0.0016
4	116	1	2.0	0.7377	2	2.0	0.2597	3	2.0	0.0016
5	153	1	2.0	0.9969	3	2.0	0.0018	4	2.0	0.0004
6	701	2	2.0	0.9922	3	2.0	0.0051	1	2.0	0.0017
7	738	2	2.0	0.7334	1	2.0	0.2582	3	2.0	0.0071
8	757	2	2.0	0.7435	1	2.0	0.2550	3	2.0	0.0005
9	859	2	2.0	0.6365	1	2.0	0.3598	3	2.0	0.0023
10	859	2	2.0	0.6386	1	2.0	0.3580	3	2.0	0.0019
SSCASPT2										
1	0	1	2.0	0.7237	2	2.0	0.2750	6	1.0	0.0003
2	0	1	2.0	0.7237	2	2.0	0.2750	6	1.0	0.0003
3	166	1	2.0	0.8471	2	2.0	0.1502	3	2.0	0.0014
4	168	1	2.0	0.8496	2	2.0	0.1479	3	2.0	0.0015
5	324	1	2.0	0.9970	3	2.0	0.0018	4	2.0	0.0003
6	344	2	2.0	0.9917	3	2.0	0.0056	1	2.0	0.0018
7	487	2	2.0	0.8448	1	2.0	0.1463	3	2.0	0.0077
8	518	2	2.0	0.8467	1	2.0	0.1516	3	2.0	0.0008
9	671	2	2.0	0.7220	1	2.0	0.2743	3	2.0	0.0024
10	672	2	2.0	0.7244	1	2.0	0.2723	3	2.0	0.0019
MSCASPT2										
1	0	1	2.0	0.7281	2	2.0	0.2705	6	1.0	0.0003
2	0	1	2.0	0.7282	2	2.0	0.2705	6	1.0	0.0003
3	146	1	2.0	0.8515	2	2.0	0.1458	3	2.0	0.0014
4	151	1	2.0	0.8542	2	2.0	0.1433	3	2.0	0.0015
5	232	1	2.0	0.9970	3	2.0	0.0018	4	2.0	0.0003
6	486	2	2.0	0.9917	3	2.0	0.0056	1	2.0	0.0017
7	554	2	2.0	0.8494	1	2.0	0.1417	3	2.0	0.0077
8	588	2	2.0	0.8511	1	2.0	0.1472	3	2.0	0.0008
9	722	2	2.0	0.7264	1	2.0	0.2698	3	2.0	0.0024
10	723	2	2.0	0.7289	1	2.0	0.2679	3	2.0	0.0019

(**3**) $[Fe(N(SiMe_3)_2)_2(AsPh_3)]$

SO State	energy [cm^{-1}]	Spin–free state	Spin	Weights	Spin–free state	Spin	Weights	Spin–free state	Spin	Weights
CASSCF										
1	0	1	2.0	0.6222	2	2.0	0.3763	6	1.0	0.0003
2	0	1	2.0	0.6217	2	2.0	0.3769	6	1.0	0.0003
3	158	1	2.0	0.7425	2	2.0	0.2532	3	2.0	0.0032
4	164	1	2.0	0.7121	2	2.0	0.2847	3	2.0	0.0022
5	264	1	2.0	0.9928	3	2.0	0.0044	2	2.0	0.0018
6	444	2	2.0	0.9946	3	2.0	0.0030	1	2.0	0.0010
7	535	2	2.0	0.7365	1	2.0	0.2557	3	2.0	0.0065
8	560	2	2.0	0.7179	1	2.0	0.2805	4	2.0	0.0005
9	710	2	2.0	0.6203	1	2.0	0.3756	3	2.0	0.0024
10	710	2	2.0	0.6204	1	2.0	0.3758	3	2.0	0.0022
SSCASPT2										
1	0	1	2.0	0.5128	2	2.0	0.4858	6	1.0	0.0003
2	0	1	2.0	0.5126	2	2.0	0.4860	6	1.0	0.0003
3	172	1	2.0	0.5330	2	2.0	0.4639	3	2.0	0.0018
4	173	1	2.0	0.5056	2	2.0	0.4913	3	2.0	0.0020
5	337	1	2.0	0.9284	2	2.0	0.0675	3	2.0	0.0030
6	352	2	2.0	0.9270	1	2.0	0.0688	3	2.0	0.0031
7	504	2	2.0	0.5092	1	2.0	0.4836	3	2.0	0.0058
8	530	2	2.0	0.5273	1	2.0	0.4713	4	2.0	0.0004
9	689	2	2.0	0.5115	1	2.0	0.4849	3	2.0	0.0020
10	689	2	2.0	0.5124	1	2.0	0.4842	3	2.0	0.0018
MSCASPT2										
1	0	1	2.0	0.6716	2	2.0	0.3270	6	1.0	0.0003
2	0	1	2.0	0.6714	2	2.0	0.3272	6	1.0	0.0003
3	152	1	2.0	0.7966	2	2.0	0.2001	3	2.0	0.0018
4	157	1	2.0	0.7848	2	2.0	0.2126	3	2.0	0.0015
5	243	1	2.0	0.9960	3	2.0	0.0022	2	2.0	0.0006
6	490	2	2.0	0.9935	3	2.0	0.0040	1	2.0	0.0014
7	565	2	2.0	0.7885	1	2.0	0.2040	3	2.0	0.0061
8	593	2	2.0	0.7901	1	2.0	0.2083	3	2.0	0.0004
9	734	2	2.0	0.6701	1	2.0	0.3263	3	2.0	0.0020
10	735	2	2.0	0.6715	1	2.0	0.3252	3	2.0	0.0018

(**4**) $[Fe(N(SiMe_3)_2)_2(OPPh_3)]$

SO State	energy [cm^{-1}]	Spin–free state	Spin	Weights	Spin–free state	Spin	Weights	Spin–free state	Spin	Weights
CASSCF										
1	0	1	2.0	0.9768	2	2.0	0.0180	3	2.0	0.0039
2	5	1	2.0	0.9764	2	2.0	0.0209	3	2.0	0.0016
3	20	1	2.0	0.9866	3	2.0	0.0075	2	2.0	0.0048
4	46	1	2.0	0.9909	2	2.0	0.0061	3	2.0	0.0022
5	47	1	2.0	0.9927	3	2.0	0.0036	2	2.0	0.0029
6	2172	2	2.0	0.9808	3	2.0	0.0173	4	2.0	0.0005
7	2176	2	2.0	0.9746	3	2.0	0.0201	1	2.0	0.0039
8	2196	2	2.0	0.9876	1	2.0	0.0065	3	2.0	0.0039
9	2221	2	2.0	0.9713	1	2.0	0.0200	3	2.0	0.0067
10	2224	2	2.0	0.9755	1	2.0	0.0195	3	2.0	0.0030
SSCASPT2										
1	0	1	2.0	0.9656	2	2.0	0.0296	3	2.0	0.0035
2	4	1	2.0	0.9645	2	2.0	0.0328	3	2.0	0.0016
3	27	1	2.0	0.9833	3	2.0	0.0079	2	2.0	0.0077
4	53	1	2.0	0.9870	2	2.0	0.0098	3	2.0	0.0024
5	57	1	2.0	0.9916	3	2.0	0.0044	2	2.0	0.0032
6	1724	2	2.0	0.9875	3	2.0	0.0108	4	2.0	0.0004
7	1732	2	2.0	0.9784	3	2.0	0.0136	1	2.0	0.0067
8	1748	2	2.0	0.9857	1	2.0	0.0103	3	2.0	0.0023
9	1782	2	2.0	0.9614	1	2.0	0.0319	3	2.0	0.0048
10	1784	2	2.0	0.9637	1	2.0	0.0315	3	2.0	0.0029
MSCASPT2										
1	0	1	2.0	0.9657	2	2.0	0.0295	3	2.0	0.0035
2	4	1	2.0	0.9646	2	2.0	0.0327	3	2.0	0.0016
3	27	1	2.0	0.9834	3	2.0	0.0079	2	2.0	0.0076
4	53	1	2.0	0.9870	2	2.0	0.0098	3	2.0	0.0024
5	56	1	2.0	0.9916	3	2.0	0.0044	2	2.0	0.0032
6	1728	2	2.0	0.9875	3	2.0	0.0108	4	2.0	0.0005
7	1736	2	2.0	0.9784	3	2.0	0.0136	1	2.0	0.0067
8	1752	2	2.0	0.9857	1	2.0	0.0102	3	2.0	0.0023
9	1786	2	2.0	0.9616	1	2.0	0.0318	3	2.0	0.0048
10	1788	2	2.0	0.9638	1	2.0	0.0313	3	2.0	0.0029

(**5a**) $[Fe(N(SiMe_3)_2)_2(Py)]$

SO State	energy [cm^{-1}]	Spin–free state	Spin	Weights	Spin–free state	Spin	Weights	Spin–free state	Spin	Weights
CASSCF										
1	0	1	2.0	0.9313	2	2.0	0.0652	3	2.0	0.0022
2	2	1	2.0	0.9296	2	2.0	0.0679	3	2.0	0.0013
3	48	1	2.0	0.9743	2	2.0	0.0173	3	2.0	0.0072
4	72	1	2.0	0.9748	2	2.0	0.0219	3	2.0	0.0024
5	83	1	2.0	0.9911	3	2.0	0.0051	2	2.0	0.0029
6	1211	2	2.0	0.9926	3	2.0	0.0057	4	2.0	0.0006
7	1227	2	2.0	0.9741	1	2.0	0.0163	3	2.0	0.0082
8	1241	2	2.0	0.9747	1	2.0	0.0224	3	2.0	0.0011
9	1296	2	2.0	0.9280	1	2.0	0.0671	3	2.0	0.0031
10	1297	2	2.0	0.9288	1	2.0	0.0667	3	2.0	0.0025
SSCASPT2										
1	0	1	2.0	0.8521	2	2.0	0.1454	3	2.0	0.0013
2	1	1	2.0	0.8502	2	2.0	0.1477	3	2.0	0.0009
3	82	1	2.0	0.9466	2	2.0	0.0459	3	2.0	0.0063
4	102	1	2.0	0.9385	2	2.0	0.0582	3	2.0	0.0024
5	129	1	2.0	0.9909	3	2.0	0.0055	2	2.0	0.0027
6	788	2	2.0	0.9949	3	2.0	0.0036	4	2.0	0.0005
7	818	2	2.0	0.9480	1	2.0	0.0445	3	2.0	0.0062
8	833	2	2.0	0.9392	1	2.0	0.0586	4	2.0	0.0006
9	920	2	2.0	0.8488	1	2.0	0.1469	3	2.0	0.0025
10	920	2	2.0	0.8494	1	2.0	0.1464	3	2.0	0.0024
MSCASPT2										
1	0	1	2.0	0.8548	2	2.0	0.1426	3	2.0	0.0013
2	1	1	2.0	0.8530	2	2.0	0.1449	3	2.0	0.0009
3	81	1	2.0	0.9478	2	2.0	0.0447	3	2.0	0.0063
4	101	1	2.0	0.9400	2	2.0	0.0567	3	2.0	0.0024
5	127	1	2.0	0.9909	3	2.0	0.0054	2	2.0	0.0027
6	797	2	2.0	0.9949	3	2.0	0.0036	4	2.0	0.0005
7	827	2	2.0	0.9492	1	2.0	0.0433	3	2.0	0.0061
8	841	2	2.0	0.9407	1	2.0	0.0571	4	2.0	0.0007
9	927	2	2.0	0.8515	1	2.0	0.1441	3	2.0	0.0025
10	927	2	2.0	0.8522	1	2.0	0.1436	3	2.0	0.0023

(**5b**) $[Fe(N(SiMe_3)_2)_2(Py)]$

SO State	energy [cm^{-1}]	Spin–free state	Spin	Weights	Spin–free state	Spin	Weights	Spin–free state	Spin	Weights
CASSCF										
1	0	1	2.0	0.9372	2	2.0	0.0589	3	2.0	0.0026
2	3	1	2.0	0.9355	2	2.0	0.0619	3	2.0	0.0014
3	44	1	2.0	0.9754	2	2.0	0.0155	3	2.0	0.0080
4	69	1	2.0	0.9767	2	2.0	0.0198	3	2.0	0.0026
5	79	1	2.0	0.9905	3	2.0	0.0055	2	2.0	0.0032
6	1269	2	2.0	0.9915	3	2.0	0.0069	4	2.0	0.0005
7	1284	2	2.0	0.9747	1	2.0	0.0142	3	2.0	0.0098
8	1298	2	2.0	0.9765	1	2.0	0.0204	3	2.0	0.0013
9	1351	2	2.0	0.9335	1	2.0	0.0610	3	2.0	0.0037
10	1352	2	2.0	0.9347	1	2.0	0.0606	3	2.0	0.0029
SSCASPT2										
1	0	1	2.0	0.8766	2	2.0	0.1206	3	2.0	0.0016
2	1	1	2.0	0.8745	2	2.0	0.1232	3	2.0	0.0010
3	72	1	2.0	0.9560	2	2.0	0.0356	3	2.0	0.0072
4	93	1	2.0	0.9508	2	2.0	0.0456	3	2.0	0.0027
5	115	1	2.0	0.9902	3	2.0	0.0059	2	2.0	0.0030
6	873	2	2.0	0.9942	3	2.0	0.0043	4	2.0	0.0005
7	898	2	2.0	0.9575	1	2.0	0.0341	3	2.0	0.0071
8	913	2	2.0	0.9515	1	2.0	0.0463	4	2.0	0.0006
9	991	2	2.0	0.8730	1	2.0	0.1223	3	2.0	0.0029
10	991	2	2.0	0.8738	1	2.0	0.1218	3	2.0	0.0026
MSCASPT2										
1	0	1	2.0	0.8785	2	2.0	0.1187	3	2.0	0.0016
2	1	1	2.0	0.8765	2	2.0	0.1213	3	2.0	0.0010
3	71	1	2.0	0.9567	2	2.0	0.0349	3	2.0	0.0072
4	93	1	2.0	0.9518	2	2.0	0.0447	3	2.0	0.0026
5	114	1	2.0	0.9903	3	2.0	0.0058	2	2.0	0.0030
6	881	2	2.0	0.9942	3	2.0	0.0043	4	2.0	0.0005
7	906	2	2.0	0.9582	1	2.0	0.0334	3	2.0	0.0071
8	921	2	2.0	0.9524	1	2.0	0.0454	4	2.0	0.0006
9	998	2	2.0	0.8749	1	2.0	0.1204	3	2.0	0.0029
10	998	2	2.0	0.8757	1	2.0	0.1199	3	2.0	0.0026

(**6**) $[Fe(N(SiMe_3)_2)_2(THF)]$

SO State	energy [cm^{-1}]	Spin–free state	Spin	Weights	Spin–free state	Spin	Weights	Spin–free state	Spin	Weights
CASSCF										
1	0	1	2.0	0.9523	2	2.0	0.0440	3	2.0	0.0025
2	3	1	2.0	0.9508	2	2.0	0.0467	3	2.0	0.0013
3	37	1	2.0	0.9807	2	2.0	0.0114	3	2.0	0.0067
4	61	1	2.0	0.9827	2	2.0	0.0143	3	2.0	0.0021
5	68	1	2.0	0.9920	3	2.0	0.0043	2	2.0	0.0028
6	1467	2	2.0	0.9924	3	2.0	0.0060	4	2.0	0.0006
7	1479	2	2.0	0.9799	1	2.0	0.0105	3	2.0	0.0082
8	1491	2	2.0	0.9822	1	2.0	0.0147	3	2.0	0.0012
9	1535	2	2.0	0.9490	1	2.0	0.0460	3	2.0	0.0030
10	1536	2	2.0	0.9500	1	2.0	0.0457	3	2.0	0.0023
SSCASPT2										
1	0	1	2.0	0.9030	2	2.0	0.0941	3	2.0	0.0017
2	2	1	2.0	0.9011	2	2.0	0.0967	3	2.0	0.0010
3	61	1	2.0	0.9660	2	2.0	0.0263	3	2.0	0.0066
4	83	1	2.0	0.9635	2	2.0	0.0334	3	2.0	0.0023
5	100	1	2.0	0.9912	3	2.0	0.0051	2	2.0	0.0028
6	994	2	2.0	0.9946	3	2.0	0.0040	4	2.0	0.0005
7	1016	2	2.0	0.9673	1	2.0	0.0251	3	2.0	0.0063
8	1029	2	2.0	0.9638	1	2.0	0.0339	3	2.0	0.0006
9	1096	2	2.0	0.8996	1	2.0	0.0960	3	2.0	0.0025
10	1096	2	2.0	0.9003	1	2.0	0.0956	3	2.0	0.0022
MSCASPT2										
1	0	1	2.0	0.9046	2	2.0	0.0925	3	2.0	0.0017
2	2	1	2.0	0.9027	2	2.0	0.0951	3	2.0	0.0010
3	61	1	2.0	0.9665	2	2.0	0.0258	3	2.0	0.0066
4	83	1	2.0	0.9642	2	2.0	0.0327	3	2.0	0.0023
5	99	1	2.0	0.9912	3	2.0	0.0050	2	2.0	0.0028
6	1004	2	2.0	0.9946	3	2.0	0.0040	4	2.0	0.0005
7	1025	2	2.0	0.9678	1	2.0	0.0246	3	2.0	0.0063
8	1038	2	2.0	0.9645	1	2.0	0.0333	3	2.0	0.0006
9	1104	2	2.0	0.9012	1	2.0	0.0944	3	2.0	0.0025
10	1105	2	2.0	0.9019	1	2.0	0.0940	3	2.0	0.0022

(**7**) $[Fe(N(SiMe_3)_2)_2(PCy_3)]$

SO State	energy [cm^{-1}]	Spin–free state	Spin	Weights	Spin–free state	Spin	Weights	Spin–free state	Spin	Weights
CASSCF										
1	0	1	2.0	0.6310	2	2.0	0.3674	3	2.0	0.0003
2	0	1	2.0	0.6304	2	2.0	0.3681	6	1.0	0.0003
3	153	1	2.0	0.7558	2	2.0	0.2385	3	2.0	0.0045
4	160	1	2.0	0.7235	2	2.0	0.2724	3	2.0	0.0030
5	255	1	2.0	0.9905	3	2.0	0.0061	2	2.0	0.0024
6	447	2	2.0	0.9926	3	2.0	0.0045	1	2.0	0.0015
7	533	2	2.0	0.7489	1	2.0	0.2404	3	2.0	0.0094
8	562	2	2.0	0.7301	1	2.0	0.2683	4	2.0	0.0005
9	708	2	2.0	0.6285	1	2.0	0.3664	3	2.0	0.0035
10	709	2	2.0	0.6288	1	2.0	0.3664	3	2.0	0.0031
SSCASPT2										
1	0	1	2.0	0.5229	2	2.0	0.4756	6	1.0	0.0003
2	0	1	2.0	0.5226	2	2.0	0.4760	6	1.0	0.0003
3	169	1	2.0	0.5679	2	2.0	0.4277	3	2.0	0.0033
4	170	1	2.0	0.5335	2	2.0	0.4625	3	2.0	0.0028
5	320	1	2.0	0.9732	2	2.0	0.0196	3	2.0	0.0062
6	360	2	2.0	0.9762	1	2.0	0.0191	3	2.0	0.0035
7	497	2	2.0	0.5580	1	2.0	0.4315	3	2.0	0.0092
8	529	2	2.0	0.5428	1	2.0	0.4558	4	2.0	0.0004
9	685	2	2.0	0.5212	1	2.0	0.4741	3	2.0	0.0032
10	685	2	2.0	0.5205	1	2.0	0.4750	3	2.0	0.0029
MSCASPT2										
1	0	1	2.0	0.7046	2	2.0	0.2939	6	1.0	0.0003
2	0	1	2.0	0.7043	2	2.0	0.2942	6	1.0	0.0003
3	142	1	2.0	0.8348	2	2.0	0.1609	3	2.0	0.0030
4	148	1	2.0	0.8235	2	2.0	0.1733	3	2.0	0.0022
5	222	1	2.0	0.9945	3	2.0	0.0035	2	2.0	0.0008
6	523	2	2.0	0.9904	3	2.0	0.0066	1	2.0	0.0019
7	585	2	2.0	0.8267	1	2.0	0.1620	3	2.0	0.0100
8	619	2	2.0	0.8266	1	2.0	0.1715	3	2.0	0.0008
9	750	2	2.0	0.7021	1	2.0	0.2930	3	2.0	0.0034
10	751	2	2.0	0.7044	1	2.0	0.2914	3	2.0	0.0028

Table S6 Effective Spin Hamiltonian parameters for the lowest pseudo spin multiplett (S = 2) of **1**–**7** from RASSI wave functions (Table S4) [a]

	1			**2**			**3**		
	CAS	SSPT2	MSPT2	CAS	SSPT2	MSPT2	CAS	SSPT2	MSPT2
D [cm^{-1}]	–36.88	–69.95	–54.27	–58.79	–49.87	–49.39	–60.54	–72.5	–56.77
E [cm^{-1}]	2.95	0.34	0.75	0.70	0.63	0.62	0.80	0.20	0.73
$g1$	1.95	1.70	1.89	1.85	1.92	1.93	1.83	1.69	1.87
$g2$	2.07	1.77	1.92	1.87	1.93	1.93	1.91	1.75	1.92
$g3$[b]	2.69	3.00	2.88	3.01	2.90	2.89	3.09	3.16	3.04

	4			**5a**			**5b**		
	CAS	SSPT2	MSPT2	CAS	SSPT2	MSPT2	CAS	SSPT2	MSPT2
D [cm^{-1}]	+11.06[c]	+12.48[c]	+12.46[c]	–19.53	–31.16	–30.81	–18.23	–27.66	–27.42
E [cm^{-1}]	2.39	3.83	3.82	3.90	3.12	3.14	4.09	3.47	3.48
$g1$	2.25	1.99	1.99	1.99	1.96	1.96	1.99	1.97	1.97
$g2$	2.17	2.14	2.14	2.12	2.09	2.09	2.13	2.11	2.11
$g3$[b]	2.00	2.31	2.31	2.44	2.64	2.63	2.42	2.58	2.58

	6			**7**		
	CAS	SSPT2	MSPT2	CAS	SSPT2	MSPT2
D [cm^{-1}]	–15.54	–23.89	–23.67	–58.83	–69.8	–52.41
E [cm^{-1}]	4.00	3.60	3.61	1.36	0.55	1.17
$g1$	1.99	1.98	1.98	1.83	1.71	1.90
$g2$	2.12	2.11	2.11	1.95	1.81	1.95
$g3$[b]	2.36	2.51	2.51	2.85	2.91	2.77

[a] Note that these parameters may be less meaningful because of the quasi-degeneracy found in complexes **1**–**3** and **7**.

[b] Note that g is given with respect to the principal axis of the g-tensor, i. e. only in axial systems (D<<0) the relation $g_3 = g_z$ holds.

[c] The sign of the calculated D becomes ambiguous in the limit of extreme rhombicity ($E/D \rightarrow 1/3$).

Table S7 Main values of the *g*-tensor and orientation of the corresponding magnetic main axes for the lowest pseudo spin multiplett a) $S = 2$ and b) $S = 1/2$ of **1**–**7** (MSPT2; Table S4, S5).[a]

a)

	g_x	g_y	g_z	Φ_1	Φ_2
1	1.89	1.92	2.88	89.5	93.7
2	1.93	1.93	2.89	90.6	94.8
3	1.87	1.92	3.04	89.5	77.5
4	1.99	2.14	2.31	88.6	82.2
5a	1.96	2.09	2.63	90.4	89.6
5b	1.97	2.11	2.58	89.2	90.0
6	1.98	2.11	2.51	88.4	89.9
7	1.90	1.95	2.77	90.1	85.4

b)

	g_x	g_y	g_z	Φ_1	Φ_2
1	0	0	11.05	89.5	93.7
2	0	0	11.17	90.4	93.8
3	0	0	11.54	89.6	82.1
4	0	0	8.85	89.4	87.7
5a	0	0	10.36	90.4	89.6
5b	0	0	10.16	89.2	90.0
6	0	0	9.90	88.4	89.9
7	0	0	10.71	90.1	88.3

[a] the magnetic main axes is characterized by its angle Φ_1 with the normal vector of the plane defined by the coordinating ligand atoms N, N, L and the angle Φ_2 with the vector lying on the Fe–L bond according to Fig. 1.

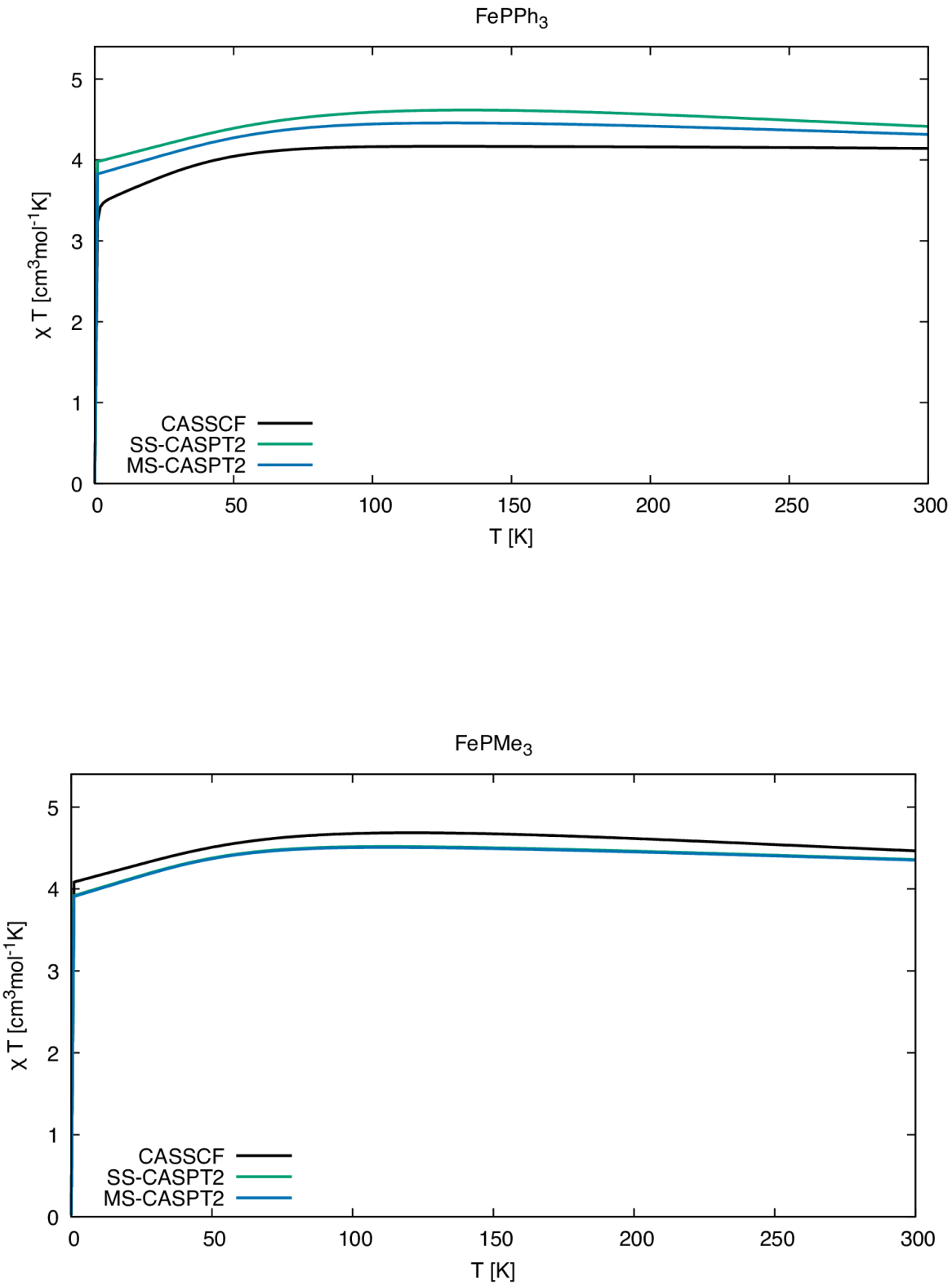

Figure S23. Temperature dependence of χT for **1** (up) and **2** (below) calculated by quantum chemical methods.

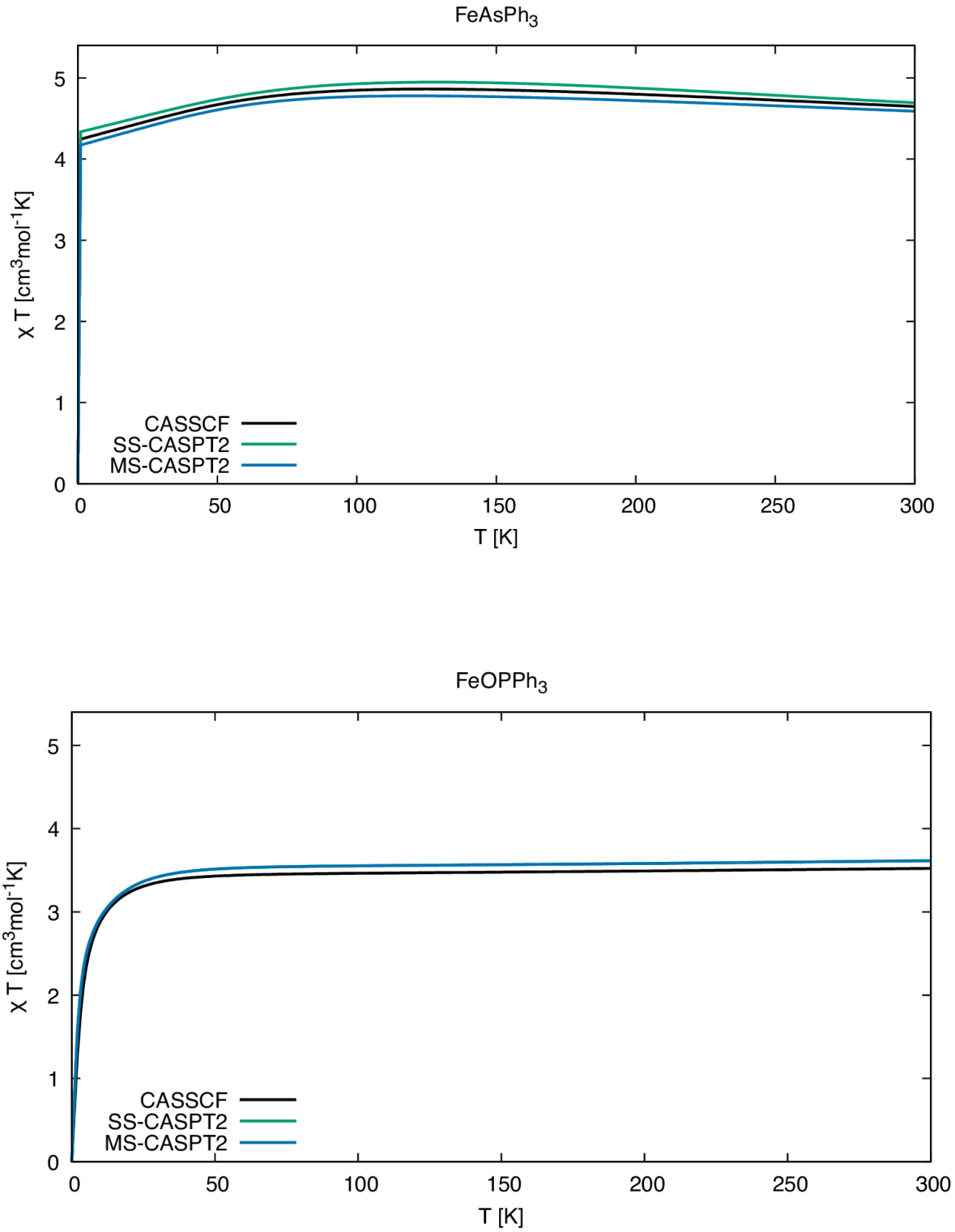

Figure S24. Temperature dependence of χT for **3** (up) and **4** (below) calculated by quantum chemical methods.

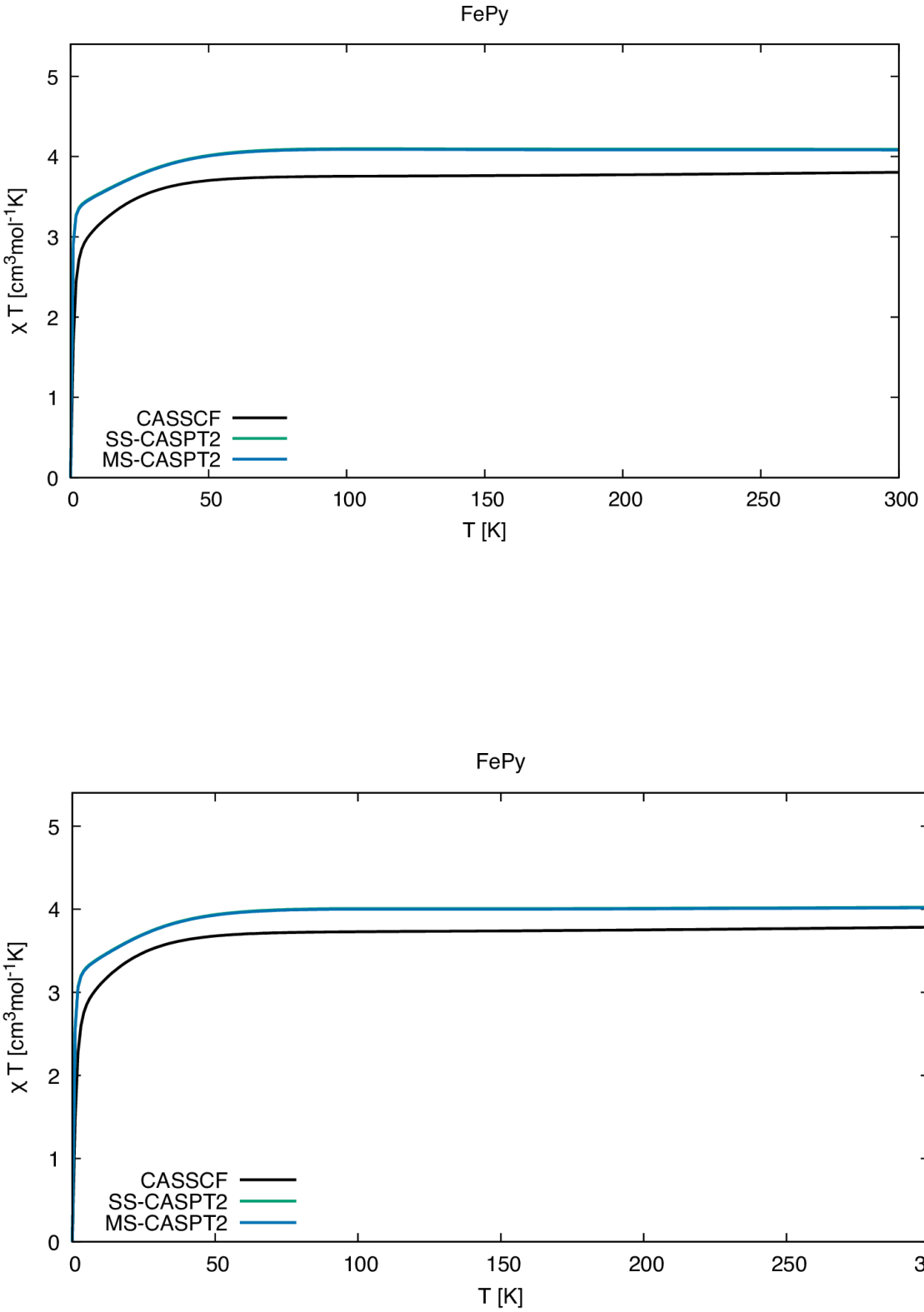

Figure S25. Temperature dependence of χT for **5a** (up) and **5b** (below) calculated by quantum chemical methods.

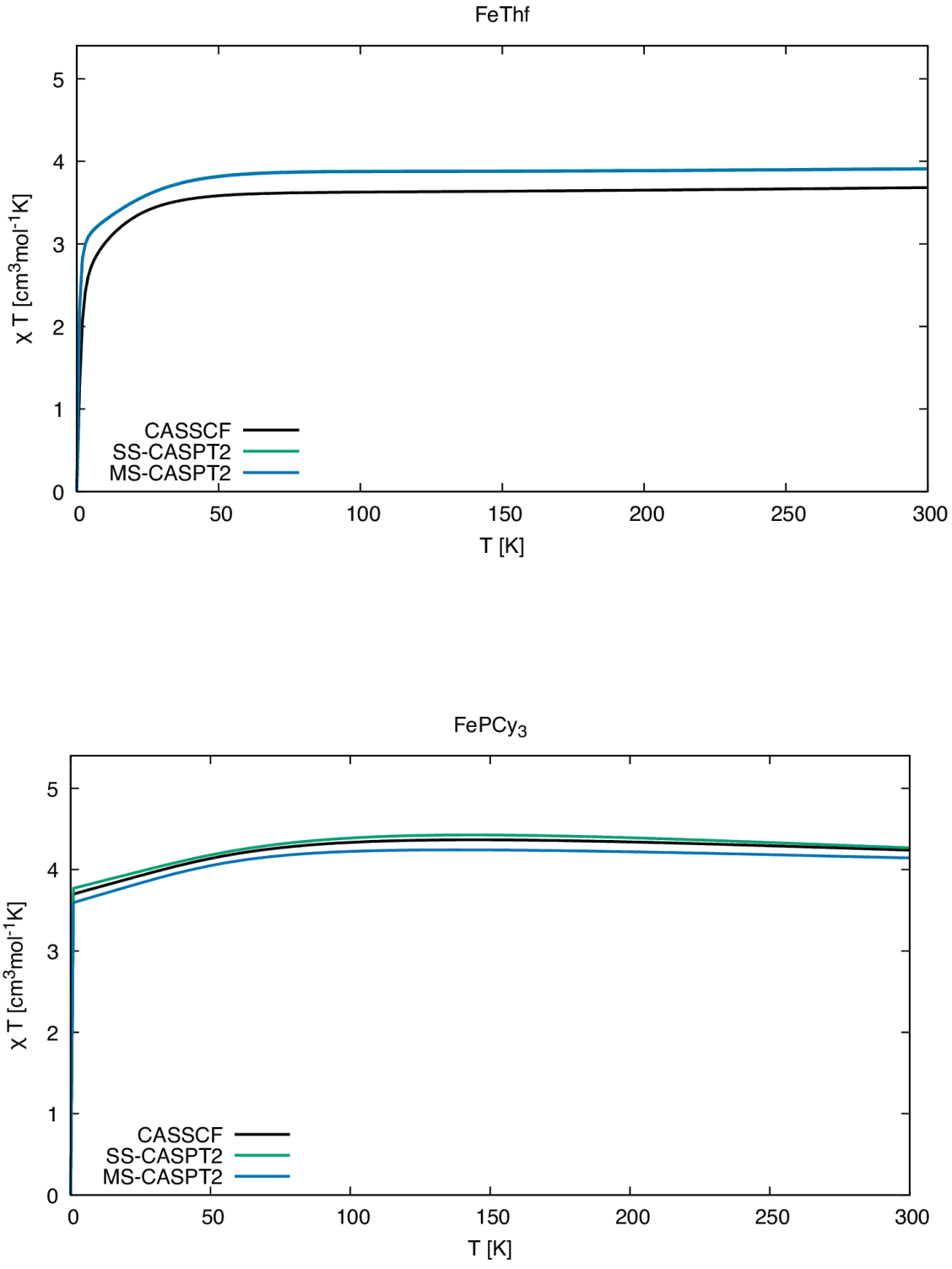

Figure S26. Temperature dependence of χT for **6** (up) and **7** (below) calculated by quantum chemical methods.

a)

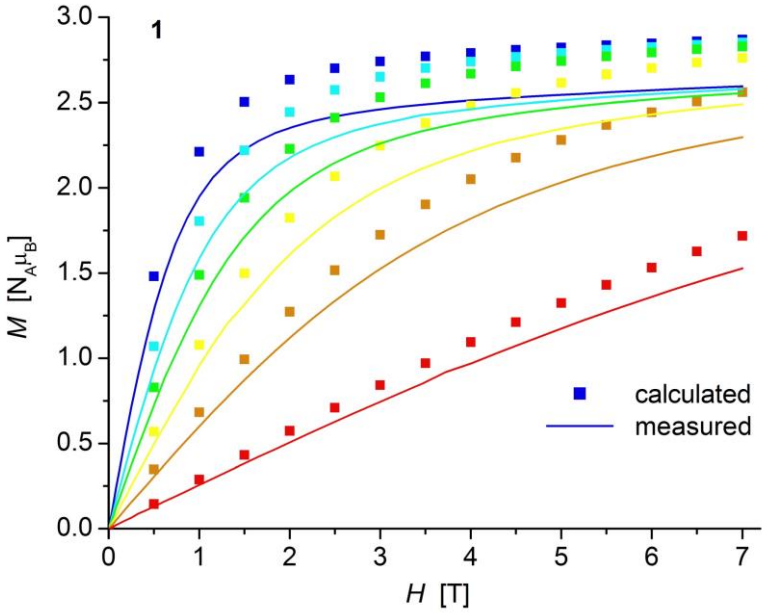

b)

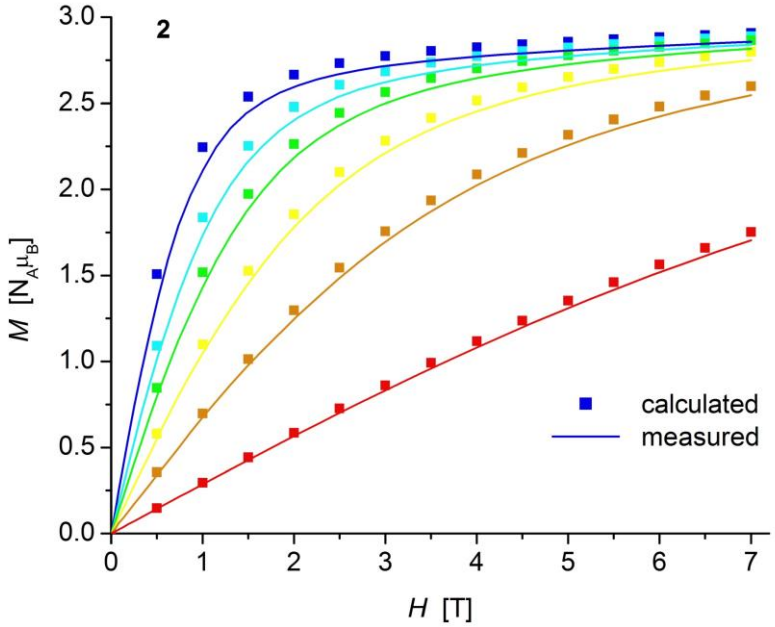

Figure S27. Comparison of the magnetization curves *M* versus *H* for a) [Fe{N(SiMe$_3$)$_2$}$_2$PPh$_3$] (**1**) and b) [Fe{N(SiMe$_3$)$_2$}$_2$PMe$_3$] (**2**) calculated by quantum chemical methods (square dots) and measured (solid line) at 2, 3, 4, 6, 10 and 25 K.

a)

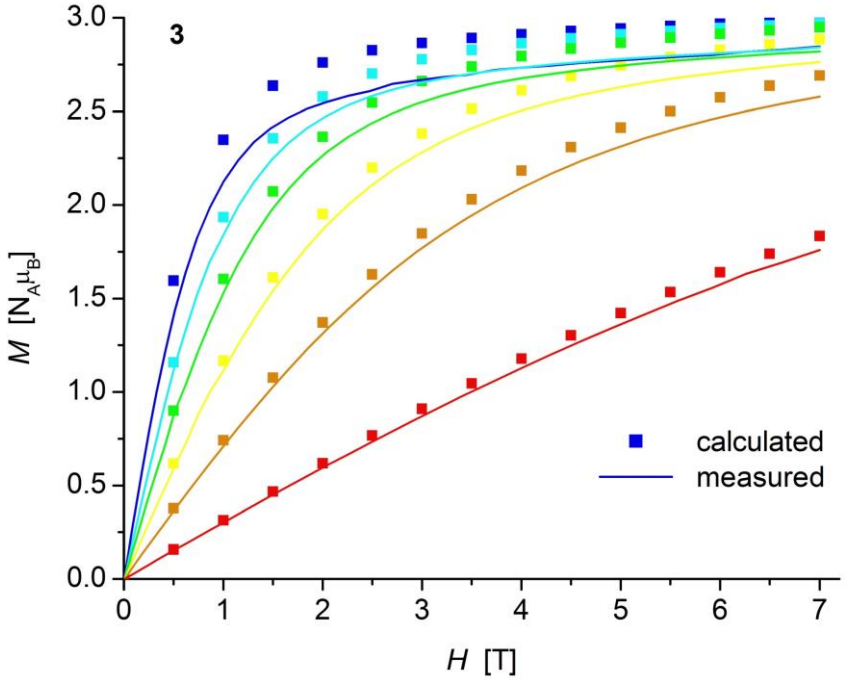

b)

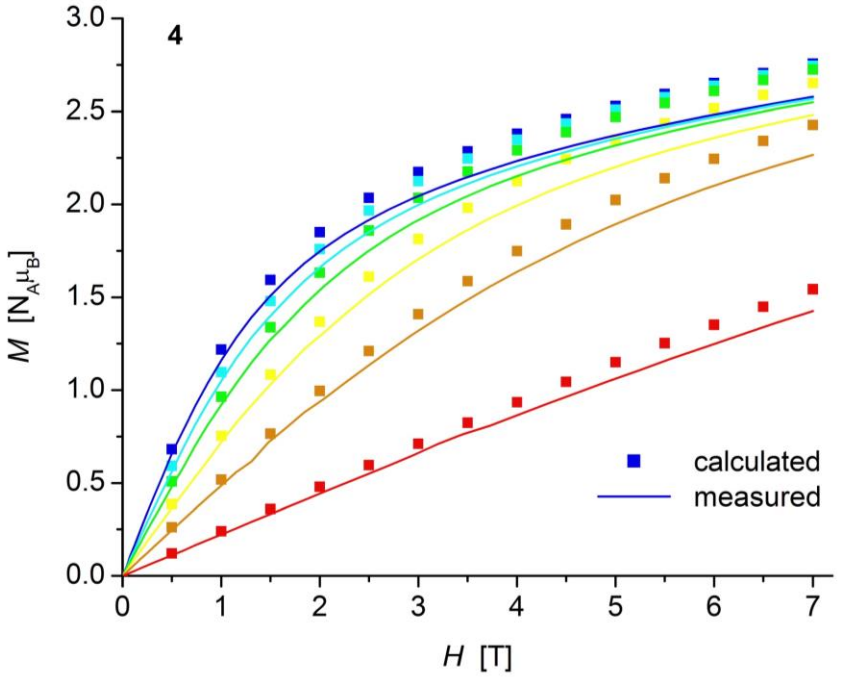

Figure S28. Comparison of the magnetization curves *M* versus *H* for a) $[Fe\{N(SiMe_3)_2\}_2AsPh_3]$ (**3**) and b) $[Fe\{N(SiMe_3)_2\}_2OPPh_3]$ (**4**) calculated by quantum chemical methods (square dots) and measured (solid line) at 2, 3, 4, 6, 10 and 25 K.

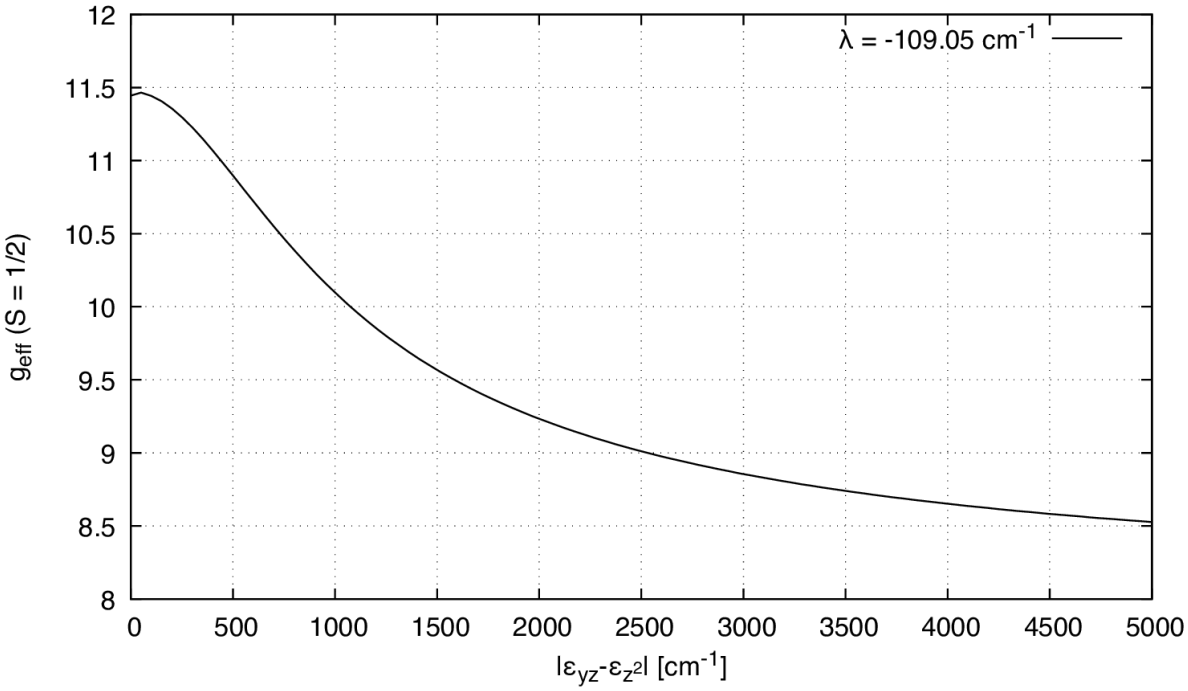

Figure S29. Relation between $g_{z'}$ and the splitting Δε according to eqn (1)†.

Table S8 d-orbital splittings of **1**–**7** derived from different quantum chemical methods. All energies are given in cm^{-1} [a]

		CAS(5,5)SCF [b]	CAS(6,5)CI [c]	CAS(6,5)SCF [d]	CAS(12,13)SCF [e]	TDDFT [f]
		LF	LF+d-d	LF+d-d+rel.		
1	d_{yz}	0	0	0	0	0
	d_{z2}	693	514	378	540	1564
	d_{xz}	3823	3277	3389	3218	5050
	d_{xy}	83778	8060	7969	8316	10221
	d_{x2-y2}	10227	10439	10345	10978	12643
2	d_{yz}	0	0	0	0	0
	d_{z2}	2398	630	491	192	2003
	d_{xz}	3319	3464	3587	4046	5380
	d_{xy}	8615	8124	8053	8420	10506
	d_{x2-y2}	9876	11360	11249	11446	14158
3	d_{yz}	0	0	0	0	0
	d_{z2}	636	567	448	176	1722
	d_{xz}	5705	3681	3806	3725	4833
	d_{xy}	7777	8088	8028	7692	10125
	d_{x2-y2}	10107	10421	10269	10357	12946
4	d_{yz}	633	560	746	2133	3247
	d_{z2}	0	0	0	0	0
	d_{xz}	2685	2487	2746	3519	5609
	d_{xy}	9385	8405	8570	9414	9937
	d_{x2-y2}	11348	10334	10473	11767	11529
5a	d_{yz}	585	195	234	1123	1580
	d_{z2}	0	0	0	0	0
	d_{xz}	3088	2750	2957	3468	5523
	d_{xy}	8149	7619	7698	8253	9596
	d_{x2-y2}	11553	11175	11190	12244	12943

5b	d_{yz}	433	62	256	1191	1367
	d_{z2}	0	0	0	0	0
	d_{xz}	2680	2459	2751	3318	5266
	d_{xy}	7299	8089	8235	8783	10307
	d_{x2-y2}	10487	11224	11335	12432	13072
6	d_{yz}	48	197	378	1395	2600
	d_{z2}	0	0	0	0	0
	d_{xz}	2870	2819	3107	3657	5860
	d_{xy}	8630	7996	8163	8801	9722
	d_{x2-y2}	10964	10303	10373	11346	11432
7	d_{yz}	0	0	0	0	0
	d_{z2}	1723	525	391	187	1722
	d_{xz}	3712	2993	3076	3166	4833
	d_{xy}	7005	8025	7930	7529	10125
	d_{x2-y2}	10180	10129	10084	10785	12946

[a] The CAS values were obtained from energies and occupation of the natural orbitals constructed for the five lowest roots. The TDDFT values were obtained from the Jacobian constructed by considering single excitations on top of the ground state.

[b] CAS(5,5)SCF: calculations performed on a Mn(II) (d^5) equivalent to eliminate d-d-correlation effects. These calculations therefore only contain ligand field effects.

[c] CAS(6,5)CI: based on CAS(5,5)SCF orbitals, theses Fe(II) calculations account additionally for correlation within the 3d shell.

[d] CAS(6,5)SCF: same as CAS(6,5)CI, but with relaxed orbitals.

[e] CAS(12,13)PT2: reference values including both static and dynamic correlation based on multi-reference wave functions.

[f] TDDFT: reference values including both dynamical and static correlation to some extent by means of the B3-LYP functional.TDDFT values of **1**–**3** and **7** are unreliable due to quasi-degeneracy.

Table S9 Coefficients of the crystal field Hamiltonian decomposition (eqn (1)) for complexes **1**–**7** (in cm^{-1})

B(k,q)	**1**	**2**	**3**	**4**	**5a**	**5b**	**6**	**7**
2,–2	–29	19	–45	–7	–11	0	0	15
2,–1	118	–79	–164	–212	56	0	0	–14
2,0	742	780	715	811	809	851	783	739
2,1	4	198	–33	155	–86	–36	24	–182
2,2	–521	–537	–597	–278	–375	–350	–363	–471
4,–4	8	–4	0	30	–8	0	0	–4
4,–3	52	–14	–44	–6	14	0	0	–5
4,–2	4	2	5	6	2	0	0	1
4,–1	13	–4	–13	–14	–6	0	0	5
4,0	10	11	9	6	8	10	6	10
4,1	–14	21	12	12	4	5	17	–11
4,2	9	18	8	16	21	16	24	12
4,3	108	–111	–115	–135	–112	1	–193	115
4,4	85	119	75	70	142	125	87	77

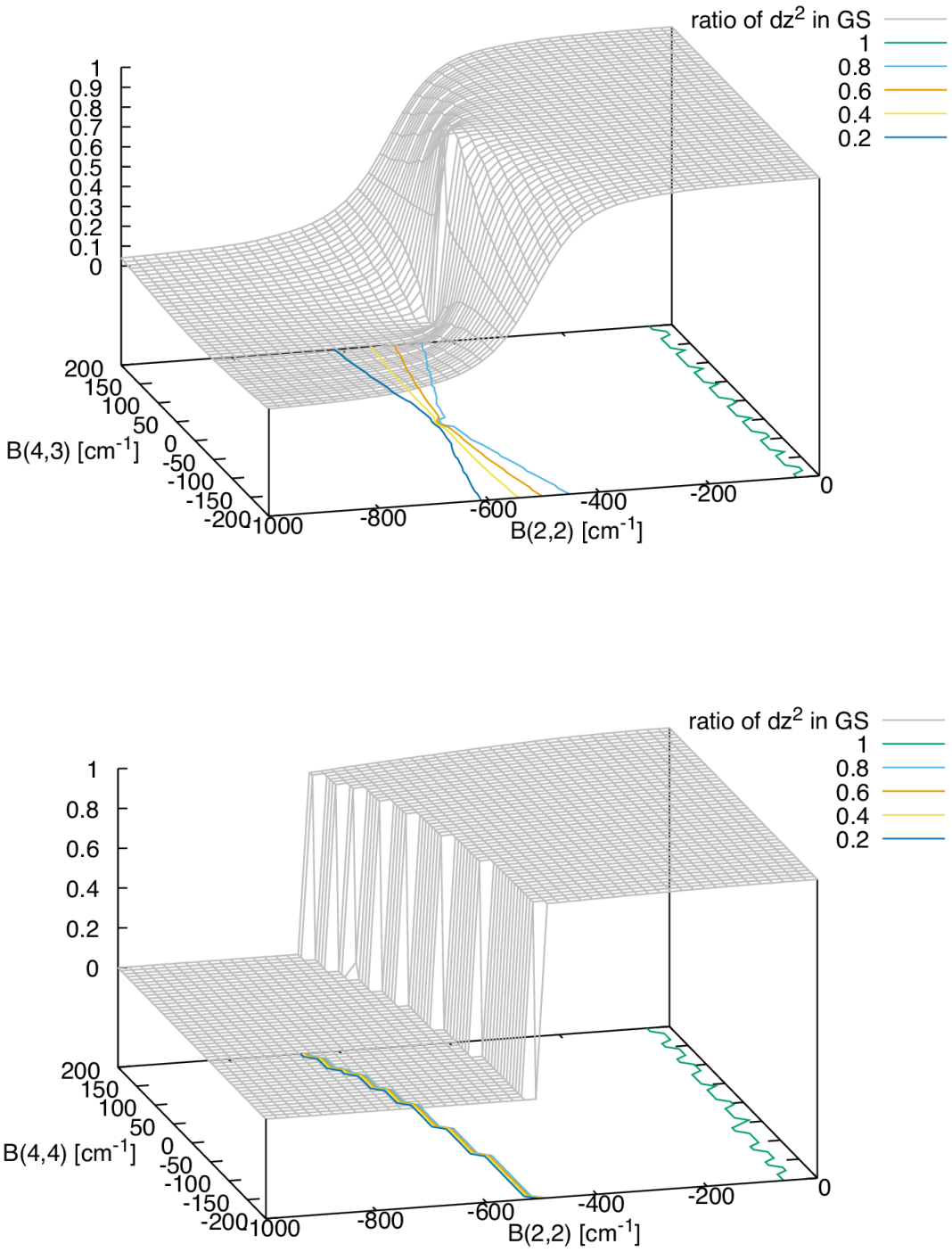

Figure S30. Simulation of the influence of B_2^2 and B_4^3 parameters (up) as well as B_2^2 and B_4^4 parameters (below) in the effective Hamiltonian eqn (1) on the symmetry of its ground state for fixed axial parameters $B_2^0 = 779$ cm^{-1} and $B_4^0 = 9$ cm^{-1} (Table S9).

Table S10 Eigenvalues E (in cm^{-1}) of the Spin Hamiltonian (eqn (3)) for $S = 2$ with D and E taken from Table 7.

	E				
1	0	0	161	165	217
2	0	0	146	150	198
3	0	0	168	173	227
4	0	4	27	53	57
5a	0	1	84	103	125
5b	0	1	73	94	112
6	0	2	62	83	98
7	0	0	154	161	210

References

(1) N. F. Chilton, R. P. Anderson, L. D. Turner, A. Soncini and K. S. Murray, *J. Comput. Chem*., 2013, **34**, 1164-1175.

(2) Aubin, S. M. J.; Sun, Z. M.; Pardi, L.; Krzystek, J.; Folting, K.; Brunel, L. C.; Rheingold, A. L.; Christou, G.; Hendrickson, D. N. *Inorg. Chem.* 1999, **38**, 5329.

(3) Atanasov, M.; Zadrozny, Long, J. R.; Neese, F.; *Chem. Sci*, 2013, **4**, 139-156.

(4) A. Fort, A. Rettori, J. Villain, D. Gatteschi, R. Sessoli, *Phys. Rev. Lett*. 1998, **80**, 612.

(5) R. L. Carlin, A. J. Duyneveldt, Magnetic Properties of Transition Metal Compounds, Springer, Berlin, Heidelberg, New York, 1977.

(6) P.-A. Lindgård, *J. Phys. C: Solid State Physics*, 1975, **8**(20), 3401–3407.